AWARD NUMBER: W81XWH-18-1-0516

TITLE: Impact of Tau Protein Deposition in Parkinson's Disease

PRINCIPAL INVESTIGATOR: Gomperts, Stephen

CONTRACTING ORGANIZATION: Massachusetts General Hospital, Boston, MA

REPORT DATE: June 2023

TYPE OF REPORT: Final

PREPARED FOR: U.S. Army Medical Research and Development Command
Fort Detrick, Maryland 21702-5012

REPORT DOCUMENTATION PAGE

Form Approved
OMB No. 0704-0188

1. REPORT DATE	2. REPORT TYPE	3. DATES COVERED
June 2023	Final	15 Aug 2018 – 14 Feb 2023

4. TITLE AND SUBTITLE

Impact of Tau Protein Deposition in Parkinson's Disease

5a. CONTRACT NUMBER

5b. GRANT NUMBER
W81XWH-18-1-0516

5c. PROGRAM ELEMENT NUMBER

6. AUTHOR(S)

Stephen Gomperts, MD, PhD, John Growdon, MD, Keith Johnson, MD, Joseph Locascio, PhD

E-Mail: sgomperts@partners.org

5d. PROJECT NUMBER

5e. TASK NUMBER

5f. WORK UNIT NUMBER

7. PERFORMING ORGANIZATION NAME(S) AND ADDRESS(ES)

Massachusetts General
Hospital
Boston, Massachusetts 02114-
2554

8. PERFORMING ORGANIZATION REPORT NUMBER

9. SPONSORING / MONITORING AGENCY NAME(S) AND ADDRESS(ES)

U.S. Army Medical Research and Development Command
Fort Detrick, Maryland 21702-5012

10. SPONSOR/MONITOR'S ACRONYM(S)

11. SPONSOR/MONITOR'S REPORT NUMBER(S)

12. DISTRIBUTION / AVAILABILITY STATEMENT

Approved for Public Release; Distribution Unlimited

13. SUPPLEMENTARY NOTES

14. ABSTRACT

A cohort of cognitively normal Parkinson's disease (PD), cognitively impaired PD, and dementia with Lewy bodies (DLB) subjects were recruited and underwent MRI, amyloid PET, and tau PET imaging, together with cognitive testing and neurological evaluation. Participants were assessed at baseline and after at least one year. There was a significant overlap in the regional pattern of cortical thinning between DLB and PDD, extending beyond the Alzheimer's signature to include the fusiform and precentral gyrus. Regional thinning was detectable in amyloid negative DLB but not cognitively impaired PD. Amyloid deposition was associated with increased cortical atrophy in both DLB and cognitively impaired PD. Across diagnostic groups, baseline amyloid burden was associated with faster longitudinal cognitive decline but was not related to longitudinal cortical thinning. Baseline tau burden was associated with longitudinal cognitive decline but was not related to longitudinal cortical thinning. Longitudinal cortical thinning was not associated with the rate of cognitive decline.

15. SUBJECT TERMS

Parkinson's disease, dementia with Lewy bodies, PET, Tau, Amyloid, PiB, AV-1451, flortaucipir, MRI

16. SECURITY CLASSIFICATION OF:			17. LIMITATION OF ABSTRACT	18. NUMBER OF PAGES	19a. NAME OF RESPONSIBLE PERSON
a. REPORT	b. ABSTRACT	c. THIS PAGE			USAMRDC
Unclassified	Unclassified	Unclassified	Unclassified	41	19b. TELEPHONE NUMBER *(include area code)*

TABLE OF CONTENTS

1. INTRODUCTION:

Alpha-synuclein deposits in Lewy bodies and neurites are the pathologic hallmark of the Lewy body diseases (LBD) - Parkinson disease (PD), PD dementia (PDD), and dementia with Lewy bodies (DLB). However, Alzheimer's disease (AD) co-pathologies in the form of extracellular beta- amyloid plaques and intracellular tau in neurofibrillary tangles (NFTs) are commonly observed in the LBD at autopsy, where they have been increasingly linked to cognitive impairment. We and others have used PET imaging with [11C]Pittsburgh Compound B (PiB) in the LBD to relate amyloid burden during life to clinical phenotype and course (1-5). In our own studies, the presence and extent of cortical amyloid in PD, PDD, or DLB was associated with faster cognitive decline (2,3). We have also employed the tau PET ligand [18F]AV-1451, also known as flortaucipir, to evaluate tau's contribution to the LBD in life, demonstrating greater cortical tau deposits in DLB and cognitively impaired PD subjects compared to cognitively normal PD and healthy subjects (6). All subjects with elevated cortical tau were cognitively impaired, and the burden of tau correlated with global measures of cognitive impairment. Surprisingly, however, and in contrast to AD, where amyloid deposition precedes cortical tau, some LBD patients with elevated tau lacked high levels of amyloid, raising the possibility that the sequence of accumulation of amyloid and tau in the LBD may diverge from AD. In this regard, how amyloid and tau deposit over time in the LBD, relate to the primary alpha-synuclein pathology of the LBD, and together contribute to the course of these diseases remain poorly understood. To address these key questions, we have set out to determine how amyloid and tau accumulate over time within LBD subjects and influence each other's deposition, whether they are associated with greater alpha-synuclein pathology, and whether they contribute to specific clinical outcomes of the LBD. We have hypothesized that tau and amyloid accumulate over time in PD and DLB, driving alpha-synuclein pathology, each other's aggregation, and cognitive impairment.

2. KEYWORDS:

Parkinson's disease (PD)
Parkinson's disease dementia (PDD)
Dementia with Lewy bodies (DLB)
Lewy body disease
Alzheimer's disease co-pathologies
Positron Emission Tomography (PET)
Tau
Amyloid
Alpha-synuclein
[11C]Pittsburgh Compound B (PiB)
[18F]AV-1451
Flortaucipir
MRI
Neurofilament light chain (NFL)
Parkinson's Progression Markers Initiative (PPMI)

3. ACCOMPLISHMENTS:

What were the major goals of the project?

Specific Aim 1. To determine whether amyloid accumulates over time within LBD subjects, and whether the presence of tau at baseline increases amyloid deposition.

Specific Aim 2. We will determine whether tau accumulates over time within LBD subjects, whether this process is influenced by baseline amyloid, and whether the longitudinal deposition of tau impacts rates of cognitive decline.

IRB approval for imaging, 1-3 months. Complete.
Patient recruitment: months 3-24. Complete.
Clinical assessments, year 1-2, months 3-24. Complete.
MRI, 1st set: months 3-12. Complete.
[11C]PiB PET, 1st set: months 3-24. Complete.
[18F]AV-1451 PET, 1st set: months 3-24. Complete.

Clinical assessments, year 2: months 12-24, 24-48. Complete.
MRI, 2nd set: months 12-48. Complete.
[11C]PiB PET, 2nd set: months 12-48. Complete.
[18F]AV-1451 PET, 2nd set: months 12-48. Complete.

Clinical assessments, year 3-4: months 24-48. Complete.
MRI, 2nd set: months 24-48. Complete.
[11C]PiB PET, 2nd set: months 24-48. Complete.
[18F]AV-1451 PET, 2nd set: months 24-48. Complete.

Data analyses:
Image processing: months 24-30. Complete.
Longitudinal PET data analyses: months 30-36. Complete.

Specific Aim 3 (modified and approved with the prior annual report): We will determine the contribution of a biofluid marker of neurodegeneration, neurofilament light chain (NFL) in blood and CSF, to progressive motor and cognitive decline in Parkinson's disease.

Acquire access to PPMI, month 18 months. Complete.
Selection of subjects from PPMI, months 18-24. Complete.
Acquire PPMI data, months 18-24. Complete.
Analyses of NFL biofluid levels: months 24-26. Complete.

What was accomplished under these goals?

Major activities: The plan of this longitudinal study is to recruit a combination of subjects without prior PET imaging (6 PD-normal, 6 PD-MCI and PDD, and 6 DLB), as well as subjects who have been imaged before (8 PD-normal, 8 PD-MCI and PDD, and 8 DLB), and to proceed with the first MRI, amyloid PET, and tau PET imaging acquisitions in 18 subjects and the first clinical assessments in all 42. The plan in years 2 and 3 is to bring in subjects for repeat imaging and proceed with data analyses, including those related to the biofluid biomarker neurofilament light chain (NFL).

- We recruited and enrolled a total of 28 new subjects for longitudinal clinical characterization and longitudinal imaging.
- We acquired 31 MR scans, 26 PiB scans, and 27 tau scans in newly recruited patients.
- We acquired 4 MR scans, 4 PiB scans, and 4 tau scans in previously imaged subjects.
- All subjects underwent detailed cognitive testing and comprehensive neurological examination.
- To improve statistical power, we incorporated data from additional subjects, including 12 sets of MRI, 8 sets of PiB, and 8 sets of tau scans.
- We published a paper focused on the impact of amyloid deposition on cortical thinning in PD, PDD, and DLB.
- We published a paper focused on the impact of CSF and blood levels of neurofilament light chain (NFL) on the progression of motor and cognitive symptoms in Parkinson's.
- The COVID-19 pandemic impacted recruitment, imaging, fluid biomarker acquisition, and clinical assessments.

Regional cortical thinning in DLB and PDD may underlie some aspect of their clinical impairments; cortical atrophy likely reflects extensive Lewy body pathology with alpha-synuclein deposits, as well as associated Alzheimer's disease co-pathologies, when present. We investigated the topographic distribution of cortical thinning in these Lewy body diseases compared to cognitively normal PD and healthy non-PD control subjects, explored the association of regional thinning with clinical features and evaluated the impact of amyloid deposition. Twenty-one participants with dementia with Lewy bodies (DLB), 16 with Parkinson disease (PD) - associated cognitive impairment (PD-MCI and PDD), and 24 cognitively normal participants with PD underwent MRI, PiB PET, and clinical evaluation. Cortical thickness across the brain and in regions of interest (ROIs) was compared across diagnostic groups and across subgroups stratified by amyloid status, and was related to clinical and cognitive measures. DLB and PD-impaired groups shared a similar distribution of cortical thinning that included regions characteristic of AD, as well as the fusiform, precentral, and paracentral gyri. Elevated PiB retention in DLB and PD-impaired but not in PD-normal participants was associated with more extensive and severe cortical thinning, in an overlapping topography that selectively affected the medial temporal lobe in DLB participants. In DLB, greater thinning in AD signature and fusiform regions was associated with greater cognitive impairment. These results show that the pattern of cortical thinning was similar in

DLB and PD-associated cognitive impairment, overlapping with and extending beyond AD signature regions to involve fusiform, precentral, and paracentral regions. Cortical thinning in AD signature and fusiform regions in these diseases reflects cognitive impairment and is markedly accentuated by amyloid co-pathology. These results raise the possibility that the distinct topography of cortical thinning in DLB and PD-associated cognitive impairment might have value as a diagnostic or outcome biomarker in clinical trials. These findings were published (Ye et al, 2020).

Across diagnostic groups, baseline amyloid burden was associated with faster longitudinal cognitive decline measured with the CDR sum of boxes score and the MOCA. Baseline amyloid burden was not related to longitudinal cortical thinning in the inferior temporal gyrus. Across diagnostic groups, baseline tau burden was associated with longitudinal cognitive decline measured with the CDR-sb (R=0.63, p=0.0051). There was a trend towards significance in the correlation of baseline tau with longitudinal change in MOCA score. Baseline tau burden was not significantly related to longitudinal cortical thinning in the inferior temporal gyrus. Longitudinal cortical thinning in the inferior temporal gyrus was not associated with the rate of cognitive decline measured with the CDR-sb (R=0.3, p=0.2). We did not detect significant accumulation of amyloid within participants (estimate mean difference across longitudinal scans = 0.03, p = 0.128) . We also did not detect accumulation of tau within participants (estimate mean difference=0.03, p = 0.363). Larger research cohorts studied over longer intervals will be needed for this purpose.

Neurofilament light chain (NFL) level in biofluids is a sensitive measure of axonal damage and a promising biomarker in neurodegenerative diseases. In PD, NFL can distinguish PD from other parkinsonian disorders, and NFL concentration is associated with disease severity, risk of progression, and survival. To determine whether serum NFL at baseline in de novo PD predicts motor decline, differentially impacts specific motor features, predicts cognitive decline, and predicts loss of dopamine terminals, we evaluated 376 de novo PD patients from the PPMI database and analyzed the effect of baseline serum NFL levels on progression over eight years of motor impairment measured with the UPDRS, cognitive function measured with the MoCA, and putamen dopamine transporter (DAT) binding ratio measured with DaTscan. In longitudinal mixed effects models that controlled for age, gender, disease duration, and levodopa equivalent drug dose, higher levels of serum NFL at baseline were associated with greater increases of UPDRS-III and total UPDRS scores, with greater worsening of postural instability and gait disorder (PIGD) scores but not tremor scores over time. In contrast, baseline serum NFL was not associated with significant progression of MoCA scores in this de novo PD cohort. Higher baseline serum NFL was associated with greater reduction of putamen DAT binding ratio over time. Together, these findings show that baseline serum NFL levels predict the rate of motor decline, the accumulation of PIGD clinical features, and the progression of dopamine transporter loss in the early stage of PD. These findings were published (Ye et al, 2021).

What opportunities for training and professional development has the project provided?

Nothing to Report.

How were the results disseminated to communities of interest?

Two manuscripts have been published.

What do you plan to do during the next reporting period to accomplish the goals?

Nothing to Report.

4. IMPACT:

What was the impact on the development of the principal discipline(s) of the project?

Our published observations support the hypothesis that accumulation of amyloid in the brain contributes to cognitive impairment in PD and DLB, driving cortical thinning and thereby cognitive deficits (8). We anticipate that these results will significantly impact research in the field, generating interest in the concept of a cortical thinning signature of these diseases and facilitating interest in working to understand the contributions of amyloid, tau, and alpha- synuclein to the clinical course of PD and DLB. Particularly with the FDA approval of amyloid clearance strategies such as lecanemab for Alzheimer's disease, our observations will contribute to gathering momentum supporting clinical trials in amyloid-positive LBD patients focused on amyloid clearance.

Our additional published observation identifying the fluid biomarker NFL as a predictor of motor decline and dopamine transporter loss in PD has also been impactful (9). Based on our results and others, we anticipate that serum NFL will become a frequently studied biomarker for clinical trials focused on neuroprotection in PD and DLB.

What was the impact on other disciplines?

Nothing to report.

What was the impact on technology transfer?

If there is nothing significant to report during this reporting period, state "Nothing to Report."

Describe ways in which the project made an impact, or is likely to make an impact, on commercial technology or public use, including:

- *transfer of results to entities in government or industry;*
- *instances where the research has led to the initiation of a start-up company; or*
- *adoption of new practices.*

Nothing to report.

What was the impact on society beyond science and technology?

Nothing to report.

5. CHANGES/PROBLEMS:

Changes in approach and reasons for change

Nothing to report.

Actual or anticipated problems or delays and actions or plans to resolve them

Delays in recruitment, imaging, and data processing due to the COVID-19 pandemic were a significant problem. We overcame these with no cost extensions.

Nothing to report.

Significant changes in use or care of human subjects, vertebrate animals, biohazards, and/or select agents

Significant changes in use or care of human subjects

Nothing to report.

Significant changes in use or care of vertebrate animals

Nothing to report.

Significant changes in use of biohazards and/or select agents

Nothing to report.

6. PRODUCTS:

- **Publications, conference papers, and presentations**

Journal publications.

Ye R, Locascio JJ, Goodheart AE, Quan M, Zhang B, Gomperts SN. Serum NFL levels predict progression of motor impairment and reduction in putamen dopamine transporter binding ratios in de novo Parkinson's disease: An 8-year longitudinal study. Parkinsonism Relat Disord. 2021;85:11-16.
Published.
Acknowledgement of federal support (yes)

Ye R, Touroutoglou A, Brickhouse M, Katz S, Growdon JH, Johnson KA, Dickerson BC, Gomperts SN. Topography of cortical thinning in the Lewy body diseases. Neuroimage Clin. 2020;26:102196. doi: 10.1016/j.nicl.2020.102196. Epub 2020 Jan 31.
Published.
Acknowledgement of federal support (yes)

Books or other non-periodical, one-time publications.

Nothing to report.

Other publications, conference papers and presentations.

Nothing to report.

- **Website(s) or other Internet site(s)**

Nothing to report.

- **Technologies or techniques**

Nothing to report.

- **Inventions, patent applications, and/or licenses**

Nothing to report.

- **Other Products**

Nothing to report.

7. PARTICIPANTS & OTHER COLLABORATING ORGANIZATIONS

What individuals have worked on the project?

Name:	Quan, Moqin
Project Role:	Research assistant
ORCID ID:	None
Nearest person month worked:	12
Contribution to Project:	Moqin Quan performed work in the area of MRI acquisition and data processing.
Funding support	NINDS and MJFF

Name:	Ye, Rong
Project Role:	Research fellow
ORCID ID:	None
Nearest person month worked:	9.69
Contribution to Project:	Rong Ye performed work in the area of data processing and analyses.
Funding support	

Name:	Gomperts, Stephen N
Project Role:	PI
ORCID ID:	0000-0002-0083-0077
Nearest person month worked:	2.71
Contribution to Project:	Stephen Gomperts provided supervision, recruitment, neurological evaluation and clinical synthesis, imaging and data analyses, and manuscript preparation.
Funding support	NINDS, NIA, MJFF, LBDA, Farmer Family Foundation Parkinson's Initiative

Has there been a change in the active other support of the PD/PI(s) or senior/key personnel since the last reporting period?

Dr. Gomperts has received new research support as a principal investigator in a grant from the NIH focused on imaging epigenetic dysregulation with the histone deacetylase PET ligand Martinostat. May 2023-April 2028. Effort 2.16 CM. Overlap, none.

Dr. Gomperts has received new research support as a co-investigator in a grant from the Michael J Fox Foundation focused on imaging alpha-synuclein with a novel PET ligand. June 2023-January 2024. Effort 1.2 CM. Overlap, none.

Dr. Gomperts has received new research support as a site investigator in a grant from the NIH focused on developing a skin biopsy diagnostic test for dementia with Lewy bodies. November 2022-March 2024. Effort 0.12 CM. Overlap, none.

Dr. Gomperts' grant from the NIH focused on amyloid's effects on hippocampal neurophysiology across the sleep-wake cycle has ended. August 2017-April 2023. Effort 2.80 CM. Overlap, none.

What other organizations were involved as partners?

Nothing to report.

8. SPECIAL REPORTING REQUIREMENTS

The QUAD Chart is attached.

9. REFERENCES

1. Gomperts, S.N., 2014. Imaging the role of amyloid in PD dementia and dementia with Lewy bodies. Curr Neurol Neurosci Rep 14, 472.
2. Gomperts, S.N., Locascio, J.J., Rentz, D., Santarlasci, A., Marquie, M., Johnson, K.A., Growdon, J.H., 2013. Amyloid is linked to cognitive decline in patients with Parkinson disease without dementia. Neurology 80, 85-91.
3. Gomperts SN, Marquie M, Locascio JJ, Bayer S, Johnson KA, Growdon JH. PET Radioligands Reveal the Basis of Dementia in Parkinson's Disease and Dementia with Lewy Bodies. Neurodegener Dis. 2016;16(1-2):118-24. doi: 10.1159/000441421. Epub 2015 Dec 8.
4. Gomperts SN, Rentz DM, Moran E, Becker JA, Locascio JJ, Klunk WE, Mathis CA, Elmaleh DR, Shoup T, Fischman AJ, Hyman BT, Growdon JH, Johnson KA. Imaging amyloid deposition in Lewy body diseases. Neurology. 2008 Sep 16;71(12):903-10.
5. Kantarci K, Lowe VJ, Boeve BF, Weigand SD, Senjem ML, Przybelski SA, Dickson DW, Parisi JE, Knopman DS, Smith GE, Ferman TJ, Petersen RC, Jack CR Jr. Multimodality imaging characteristics of dementia with Lewy bodies. Neurobiol Aging. 2012 Sep;33(9):2091-105.
6. Gomperts, S.N., Locascio, J.J., Makaretz, S.J., Schultz, A., Caso, C., Vasdev, N., Sperling, R., Growdon, J.H., Dickerson, B.C., Johnson, K., 2016. Tau Positron Emission Tomographic Imaging in the Lewy Body Diseases. JAMA Neurol 73, 1334-1341.
7. Litvan, I., Goldman, J.G., Troster, A.I., Schmand, B.A., Weintraub, D., Petersen, R.C., Mollenhauer, B., Adler, C.H., Marder, K., Williams-Gray, C.H., Aarsland, D., Kulisevsky, J., Rodriguez-Oroz, M.C., Burn, D.J., Barker, R.A., Emre, M., 2012. Diagnostic criteria for mild cognitive impairment in Parkinson's disease: Movement Disorder Society Task Force guidelines. Mov Disord 27, 349-356.
8. Ye R, Touroutoglou A, Brickhouse M, Katz S, Growdon JH, Johnson KA, Dickerson BC, Gomperts SN. Topography of cortical thinning in the Lewy body diseases. Neuroimage Clin. 2020;26:102196. doi: 10.1016/j.nicl.2020.102196. Epub 2020 Jan 31.
9. Ye R, Touroutoglou A, Brickhouse M, Katz S, Growdon JH, Johnson KA, Dickerson BC, Gomperts SN. Topography of cortical thinning in the Lewy body diseases. Neuroimage Clin. 2020;26:102196. doi: 10.1016/j.nicl.2020.102196. Epub 2020 Jan 31.

10. APPENDICES:

APPENDIX 1 – QUAD CHART

Imaging Alzheimer's Disease Pathology in Parkinson Disease and Dementia With Lewy Bodies

PD170054, Final Report
W81XWH-18-1-0516

PI: Stephen Gomperts, MD, PhD **Org:** MGH, The General Hospital Corp. **Award Amount: $999,992**

Study Aims

- Aim 1. To determine whether amyloid accumulates over time within LBD subjects, and whether the presence of tau at baseline increases amyloid deposition
- Aim 2. We will determine whether tau accumulates over time within LBD subjects, whether this process is influenced by baseline amyloid, and whether the longitudinal deposition of tau impacts rates of cognitive decline
- Aim 3. We will determine whether levels of neurofilament light chain (NFL) in CSF and blood impact the rate of motor and cognitive decline in de novo PD in the Parkinson's Progression Markers Initiative.

Approach

We will acquire baseline amyloid PET and tau PET scans and subsequent follow-up scans 2 years later, along with serial MRI, standardized neurologic exams, and detailed cognitive testing, in cognitively normal PD, PDD, and DLB subjects, leveraging our previously acquired cohort. We will relate CSF and blood NFL levels in de novo PD to motor and cognitive function.

Timeline and Cost

Activities / CY	18	19	20	21	22	23
Recruitment						
Initial imaging & cognitive testing						
Biofluid acquisition/studies						
Repeat imaging & cognitive testing						
Estimated Budget ($K)	**$329**	**$324**	**$347**	**NCE**	**NCE**	

Updated: 06/08/2023

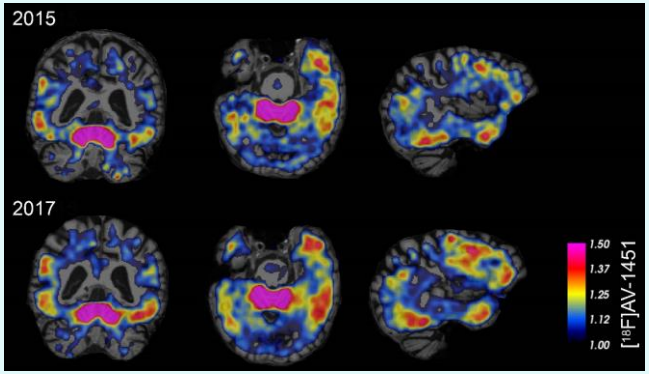

Imaging accumulation of tau and amyloid in PD and DLB. Tau PET scans for a single subject are shown.

Accomplishment: 28 new subjects and 14 previously imaged subjects were enrolled. 19 new subjects were imaged with PET and MRI. 12 previously imaged subjects underwent repeat imaging. Two manuscripts were published.

Goals/Milestones

CY18 Goal – Recruitment of new and previously imaged subjects
☑ Start recruitment
☑ Start annual cognitive and clinical testing
☑ Initial MRI, AV-1451 PET, PiB PET
☑ Genetic testing, CSF assessments

CY19 Goal – Continue data acquisition
☑ Annual cognitive and clinical testing
☑ Initial and repeat MRI, AV-1451 PET, PiB PET
☑ CSF assessments

CY20Goal – Complete imaging, data analyses
☑ Continue repeat MRI, AV-1451 PET, PiB PET
☑ CSF assessments
☑ Continue data analyses

CY21 Goal – Complete imaging, data analyses
☑ Continue repeat MRI, AV-1451 PET, PiB PET
☑ Continue data analyses

CY22 Goal – Complete imaging, data analyses
Continue repeat MRI, AV-1451 PET, PiB PET
☑ Complete MRI, AV-1451 PET, PiB PET
☑ Continue data analyses

CY23 Goal – Complete data analyses
☑ Complete data analyses

Comments/Challenges/Issues/Concerns The COVID-19 pandemic slowed subject visits.
Budget Expenditure for this quarter: Projected Expenditure: $0 Actual: $999,992.00

APPENDIX 2 – Manuscript published

NeuroImage: Clinical 26 (2020) 102196

Contents lists available at ScienceDirect

NeuroImage: Clinical

journal homepage: www.elsevier.com/locate/ynicl

Topography of cortical thinning in the Lewy body diseases

Rong Ye[a,1], Alexandra Touroutoglou[a,b,1], Michael Brickhouse[a,b], Samantha Katz[c], John H. Growdon[a], Keith A. Johnson[a,b,c], Bradford C. Dickerson[a,b], Stephen N. Gomperts[a,*]

[a] Department of Neurology, Massachusetts General Hospital, Charlestown, MA, USA
[b] Athinoula A. Martinos Center for Biomedical Imaging, Massachusetts General Hospital, Charlestown, MA, USA
[c] Department of Radiology, Massachusetts General Hospital, Boston, MA, USA

ARTICLE INFO

Keywords:
Cortical thinning
Amyloid deposition
Dementia with lewy bodies
Parkinson disease

ABSTRACT

Objective: Regional cortical thinning in dementia with Lewy bodies (DLB) and Parkinson disease dementia (PDD) may underlie some aspect of their clinical impairments; cortical atrophy likely reflects extensive Lewy body pathology with alpha-synuclein deposits, as well as associated Alzheimer's disease co-pathologies, when present. Here we investigated the topographic distribution of cortical thinning in these Lewy body diseases compared to cognitively normal PD and healthy non-PD control subjects, explored the association of regional thinning with clinical features and evaluated the impact of amyloid deposition.

Methods: Twenty-one participants with dementia with Lewy bodies (DLB), 16 with Parkinson disease (PD) - associated cognitive impairment (PD-MCI and PDD), and 24 cognitively normal participants with PD underwent MRI, PiB PET, and clinical evaluation. Cortical thickness across the brain and in regions of interest (ROIs) was compared across diagnostic groups and across subgroups stratified by amyloid status, and was related to clinical and cognitive measures.

Results: DLB and PD-impaired groups shared a similar distribution of cortical thinning that included regions characteristic of AD, as well as the fusiform, precentral, and paracentral gyri. Elevated PiB retention in DLB and PD-impaired but not in PD-normal participants was associated with more extensive and severe cortical thinning, in an overlapping topography that selectively affected the medial temporal lobe in DLB participants. In DLB, greater thinning in AD signature and fusiform regions was associated with greater cognitive impairment.

Conclusions: The pattern of cortical thinning is similar in DLB and PD-associated cognitive impairment, overlapping with and extending beyond AD signature regions to involve fusiform, precentral, and paracentral regions. Cortical thinning in AD signature and fusiform regions in these diseases reflects cognitive impairment and is markedly accentuated by amyloid co-pathology. Further work will be required to determine whether the distinct topography of cortical thinning in DLB and PD-associated cognitive impairment might have value as a diagnostic and/ or outcome biomarker in clinical trials.

1. Introduction

The Lewy body diseases—dementia with Lewy bodies (DLB), Parkinson disease dementia (PDD), and Parkinson disease (PD)—are characterized neuropathologically by neuronal inclusions of α-synuclein in cortical and subcortical regions as well as loss of neuromodulator neuronal populations including dopamine cells of the substantia nigra pars compacta and cholinergic cells of the basal forebrain (Gomperts, 2014; Halliday et al., 2014). The shared clinical features of DLB and PDD—which together comprise the Lewy body dementias (LBD)—include progressive cognitive impairment in association with parkinsonism, visual hallucinations, rapid eye movement sleep behavior disorder (RBD), and fluctuations in alertness and cognition. This clinical overlap suggests that the common neuropathology of the LBD impacts an overlapping set of vulnerable brain regions.

Imaging-based assessments of regional cortical atrophy in the LBD have provided a valuable approach to detect affected cortical regions (Song et al., 2011; Summerfield et al., 2005; Watson et al., 2015;

Abbreviations: CDR-SB, Clinical Dementia Rating Sum of Box; DLB, Dementia with Lewy bodies; H & Y, Hoehn and Yahr scale; MMSE, Mini-Mental State Examination; HC, healthy controls; PD, Parkinson disease; PiB, Pittsburgh compound B; UPDRS, Unified Parkinson Disease Rating Scale

* Corresponding author at: Department of Neurology, Building 114, 16th Street - 2004, Charlestown, MA, 02129-4404.
E-mail address: sgomperts@partners.org (S.N. Gomperts).

[1] R.Y. and A.T. contributed equally to this work.

https://doi.org/10.1016/j.nicl.2020.102196
Received 17 September 2019; Received in revised form 21 January 2020; Accepted 22 January 2020
Available online 31 January 2020

Weintraub et al., 2011). Although atrophy has been reported in both diseases, cortical volume loss is often more extensive and severe in DLB than PDD (Beyer et al., 2007; Borroni et al., 2015; Burton et al., 2004; Lee et al., 2010; Sanchez-Castaneda et al., 2009). One contributor to this distinction may be the greater prevalence and severity of concomitant Alzheimer's disease (AD)-related pathologic changes in DLB, including amyloid plaques and neurofibrillary tangles observed at autopsy (Harding and Halliday, 2001). Indeed, the presence of amyloid deposition in DLB (Gomperts, 2014) has been associated with greater cortical thinning (Lee et al., 2018; Mak et al., 2019), greater medial temporal atrophy (van der Zande et al., 2018), and a faster rate of cortical atrophy (Sarro et al., 2016). Studies aggregating patients with DLB, PDD, and the Lewy body variant of AD concur: cortical thinning was greater in the presence of amyloid and extended into widespread association cortices (Kang et al., 2019; Shimada et al., 2013). However, to our knowledge, the impact of amyloid on cortical thinning in PD and PDD has not been directly assessed.

In AD, a stereotyped topography of cortical thinning has been replicated in multiple studies; known as the “AD signature,” this distributed pattern of cortical atrophy involves heteromodal and paralimbic cortical regions known to be affected by AD neuropathology (Bakkour et al., 2009, 2013; Dickerson et al., 2009, 2011; Racine et al., 2018). In DLB, concomitant amyloid deposition evident on amyloid PET appears to drive a pattern of cortical thinning similar to AD, with additional regional thinning that may reflect the underlying synucleinopathy (Lee et al., 2018). To assess whether these observations extend to PDD and to explore how regional cortical thinning relates to clinical features of the Lewy body diseases, here we compared MR measures of cortical thinning in DLB, cognitively impaired PD and cognitively normal PD, assessed the impact of amyloid burden on the topography and severity of cortical thinning, and related regional cortical thinning to clinical features. We hypothesized that the topography of cortical thinning would be similar in DLB and cognitively impaired PD, overlapping with the “AD signature” on the basis of amyloid accumulation, with additional cortical involvement relevant to the distinguishing clinical features of the LBD. We also predicted that cortical amyloid would increase thinning in both groups, and that regional thinning in DLB and PD would relate to cognitive and motor impairments.

2. Methods

2.1. Participants and clinical assessments

Twenty-one participants with DLB, 16 PD with a broad range of cognitive impairments (PD-impaired; including 7 with PD-MCI and 9 with PDD), and 24 cognitively-normal individuals with PD (PD-normal) were recruited from Massachusetts General Hospital's Movement and Memory Disorder Units. All participants with DLB fulfilled the consortium criteria for probable DLB (McKeith et al., 2017). Participants with PD met the clinical criteria of the UK Parkinson's Disease Society Brain Bank (Hughes et al., 1993). Subjects with PD-MCI met level II Movement Disorder Society (MDS) Task Force guidelines (Litvan et al., 2012). The clinical MDS criteria for probable PDD were used for diagnosis of PDD participants (Emre et al., 2007). Subjects underwent clinical evaluation including scoring of motor function with the Unified Parkinson Disease Rating Scale part III (UPDRS-III) and detailed neuropsychological tests of the Unified Data Set of the Alzheimer's Disease Research Centers (Beekly et al., 2007; Morris et al., 2006), including the Clinical Dementia Rating Sum-of-Boxes score (CDR-SB), Mini-Mental State Examination (MMSE), Neuropsychiatric Inventory Questionnaire for assessment of hallucinations, and Mayo fluctuations scale (Ferman et al., 2004). The diagnostic groups were well matched for age (Table 1). Across all participants, the extent of concomitant small vessel disease evident on MR imaging was either absent or mild. Subjects with significant white matter hyperintensities (WMH), defined as either confluent deep WMH or irregular periventricular WMH extending into the deep white matter, were excluded. Thirty-one subjects underwent dopamine transporter PET imaging for purposes unrelated to the current study; putamen DAT concentration was reduced in all. The diagnosis of Lewy body disease was confirmed with neuropathological evaluation in all 18 cases that came to autopsy.

MR data from 115 age-matched healthy cognitively normal (CDR 0) individuals acquired in previous studies (Bickart et al., 2014; Dickerson et al., 2009; Moriguchi et al., 2011) were also employed for vertex-based and regions of interest (ROIs) - based cortical thickness analyses.

This study was approved by the Partners Human Research Committee Institutional Review Board of Partners Healthcare, Inc.

2.2. Neuroimaging procedures

Patient were scanned in an identical manner on a 3T Tim Trio (Siemens). High resolution structural T1-weighted magnetization-prepared rapid gradient-echo (MPRAGE) sequence were acquired with the following parameters: (TR = 2.3 ms, TE = 2.98 ms, flip angle = 9°, field of view = 240 mm × 256 mm, slice thickness = 1 mm and TR = 2.53 ms, TE = 1.64 ms, flip angle = 7°, field of view = 256 mm × 256 mm, slice thickness = 1 mm) processed with Freesurfer (version 6.0, freely available at http://surfer.nmr.mgh.harvard.edu). For all subjects, procedures for data collection included head movement restriction using expandable foam cushions, and automated scout and shimming procedures.

The technical details for MRI morphometric data analysis have been previously described in detail (Fischl and Dale, 2000; Fischl et al., 1999; Salat et al., 2004). In brief, for each individual subject, cortical thickness at each surface location (vertex) was measured as the average of the closest distance from the gray matter/white matter boundary to the corresponding cortical surface. The accuracy for this measurement has been validated by direct comparisons with manual measures on post-mortem brain (Rosas et al., 2002) and on MRI data (Kuperberg et al., 2003). After visual inspection for each individual subject, the cortical thickness data were smoothed along the cortical surface using a Gaussian kernel with a full width at half maximum of 15 mm.

Based on study hypotheses, we obtained cortical thickness from AD signature regions of cortical thinning (Bakkour et al., 2009; Dickerson et al., 2009). The AD signature ROIs were selected on the basis of their relevance to cognitive function and anticipated vulnerability to cortical amyloid. Cortical thickness values from these ROIs were then subjected to statistical analyses for ROIs as described below (Sections 2.3).

In addition, we obtained cortical thickness from three ROIs of the Desikan-Killiany atlas (Desikan et al., 2006) determined based on the exploratory vertex-based analysis of the statistical surface maps for the contrast of DLB vs. HC groups. These ROIs which included precentral, paracentral, and fusiform regions were anticipated to relate to clinical features in the Lewy body diseases. Cortical thickness values from these ROIs were subjected to statistical analyses for ROIs as described below (Sections 2.3). To generate the statistical surface maps, we computed a two-class general linear model for the effects of diagnostic group on cortical thickness at each point (threshold $P < 0.05$, FDR corrected).

[11C]PiB PET was acquired using a Siemens/CTI (Knoxville, TN) ECAT HR+ scanner (63 image planes; 15.2 cm axial field of view; 4.1 mm transaxial resolution and 2.4 mm slice interval) with a 8.5 to 15 mCi bolus injection followed immediately by a 60-minute dynamic acquisition in 39 frames (8 × 15 s, 4 × 60 s, 27 × 120 s). PET data were reconstructed and attenuation corrected, and each frame was evaluated to verify adequate count statistics and absence of head motion. [11C]PiB PET data were expressed as the distribution volume ratio (DVR) with cerebellar gray as reference. [11C]PiB retention was assessed using a large cortical ROI aggregate comprised of frontal, lateral temporal and retrosplenial cortices (FLR). For use as a dichotomous measure, high Aβ was defined as FLR DVR ≥ 1.32 after partial volume

Table 1
Demographic and clinical characteristics of participants.

Group	N	Sex (M/F)	Age (years)	Education (years)	Duration of Motor Impairment (years) [a, b]	Duration of Cognitive Impairment (years)	MMSE [a, b]	CDR-SB [a, b]	UPDRS-III [a]	H & Y	Hallucination [a] (N,%)
DLB	21	18/3	71.6 (7.1)	15.9 (2.6)	3.3 (1.4) [c, d]	4.8 (2.3)	20.4 (8.4) [c, d]	7.2 (5.0) [c, d]	30.9 (14.1) [d]	2.4 (0.9)	11 (52.4) [d]
Aβ $^{+}$	10	8/2	74.1 (4.1)	16.1 (2.9)	3.2 (1.4) [f]	5.3 (3.0)	17.6 (10.3) [f, g]	8.1 (5.3) [f, g]	27.5 (17.7)	2.2 (1.2)	5 (50.0)
Aβ $^{-}$	9	8/1	70.1 (9.0)	15.9 (2.6)	3.3 (1.7) [h, i]	4.2 (1.6)	23.4 (4.4) [i]	5.8 (4.0) [i, j]	31.6 (7.9)	2.4 (0.5)	5 (55.6)
PD-impaired	16	12/4	73.1 (7.2)	16.7 (2.4)	9.4 (4.7) [c]	4.4 (3.2)	24.9 (3.3) [c, e]	3.3 (2.6) [c, e]	28.0 (10.7)	2.7 (0.8)	5 (31.3) [e]
Aβ $^{+}$	7	5/2	71.6 (7.2)	16.4 (2.3)	8.4 (2.9)	4.9 (2.1)	23.3 (3.7) [k]	4.1 (3.2)	29.0 (12.4)	2.7 (0.7)	3 (42.9)
Aβ $^{-}$	9	7/2	74.2 (7.3)	16.9 (2.7)	10.2 (5.8) [f, h]	4.1 (3.9)	26.1 (2.4) [f]	2.6 (2.0) [f]	27.2 (9.8)	2.7 (0.8)	2 (22.2)
PD-normal	24	16/8	69.0 (6.9)	16.7 (2.9)	9.3 (5.4) [d]	–	29.6 (0.6) [d, e]	0.2 (0.3) [d, c]	19.8 (10.9) [d]	2.3 (0.8)	1 (4.2) d, [e]
Aβ $^{+}$	6	5/1	73.1 (6.8)	17.7 (2.0)	5.3 (2.3)	–	29.3 (0.8) [g]	0.1 (0.2) [g, j]	17.0 (9.3)	2.2 (0.3)	0 (0)
Aβ $^{-}$	18	11/7	67.6 (6.5)	16.4 (3.1)	10.6 (5.5) [f, i]	–	29.7 (0.5) [f, i, k]	0.2 (0.3) [f, i]	20.8 (11.5)	2.3 (0.9)	1 (5.6)
HC	115	–	69.4 (7.4)	–	–	–	–	–	–	–	–

Abbreviations: CDR-SB, Clinical Dementia Rating Sum of Box; DLB, Dementia with Lewy bodies; H & Y, Hoehn and Yahr stage; MMSE, Mini-Mental State Examination; HC, healthy controls; PD, Parkinson disease; PiB, Pittsburgh compound B; UPDRS, Unified Parkinson Disease Rating Scale.
Values represent mean (standard deviation) unless otherwise noted. Group analyses were tested among DLB, PD-impaired, and PD-normal groups. Subgroup differences were tested among amyloid positive and negative DLB, PD-impaired and PD-normal groups. Average ages of all groups, subgroups and HC were similar. Note that amyloid status of two DLB participants was unknown; they were not included in subsequent subgroup analyses.

[a] Between group difference, $p < 0.05$, ANOVA; for analysis of hallucination, $p < 0.05$, Chi square test.
[b] Between subgroup difference, $p < 0.05$, ANOVA.
[c] DLB vs. PD-impaired, $p < 0.05$, Tukey's post hoc test.
[d] DLB vs. PD-normal, $p < 0.05$, Tukey's post hoc test; for analysis of hallucination, $p < 0.05$, Chi square test.
[e] PD-impaired vs. PD-normal, $p < 0.05$, Tukey's post hoc test; for analysis of hallucination, $p < 0.05$, Chi square test.
[f] Amyloid-positive DLB vs. amyloid-negative PD-impaired, amyloid-positive DLB vs. amyloid-negative PD-normal, $p < 0.05$, Tukey's post hoc test.
[g] Amyloid-positive DLB vs. amyloid-positive PD-normal, $p < 0.05$, Tukey's post hoc test.
[h] Amyloid-negative DLB vs. amyloid-negative PD-impaired, $p < 0.05$, Tukey's post hoc test.
[i] amyloid-negative DLB vs. amyloid-negative PD-normal, $p < 0.05$, Tukey's post hoc test.
[j] amyloid-negative DLB vs. amyloid-positive PD-normal, $p < 0.05$, Tukey's post hoc test.
[k] amyloid-positive PD-impaired vs. amyloid-negative PD-normal, $p < 0.05$, Tukey's post hoc test.

correction using SGTM (Greve et al., 2016), based on a Gaussian mixture model on a reference dataset of clinically normal elderly (Mormino et al., 2014). In three participants, amyloid status was made either via visual assessment (PiB negative, $n = 1$ DLB) or autopsy (Aβ negative, A1B1C1, $n = 1$ DLB; Aβ positive, A3B2C2, $n = 1$ PDD) (Hyman et al., 2012). Two DLB subjects lacked [11C]PiB scans or autopsy results and were excluded from amyloid subgroup analyses.

To examine the effect of amyloid deposition on cortical thinning in LBD, we stratified DLB and PD-impaired subjects by amyloid status (+/-). In vertex-based analysis, we generated statistical surface maps by computing a two-class general linear model comparing healthy controls with amyloid-positive DLB, amyloid-negative DLB, amyloid-positive PD-impaired and amyloid-negative PD-impaired groups. In ROIs analysis, the AD signature regions and the three additional ROIS (fusiform, precentral and paracentral) were subjected to statistical analyses as described below (Sections 2.3).

2.3. Statistical analysis

Group statistical comparisons were performed using analysis of variance with post hoc pairwise comparisons for continuous measures or χ^2 for proportions. In ROI analyses, Bonferroni correction was used for comparisons across multiple ROIs. Relationships between continuous measures (e.g., between regional anatomic measures and the severity of clinical symptoms) were assessed with Spearman correlations, adjusting for age. Statistical analyses were conducted using R Software (version 3.3.3, freely available at https://www.r-project.org/).

3. Results

3.1. Clinical characteristics

Participant characteristics are presented in Table 1. The DLB, PD-impaired and PD-normal groups did not differ on the basis of age, years of education, or sex, which was skewed toward men in all disease groups. Cognitive impairment measured with MMSE and CDR-SB scores was greater in DLB than in the PD-impaired group (for each contrast, Tukey's post hoc t-test, $p < 0.05$). Motor impairments assessed with the UPDRS motor subscale and Hoehn and Yahr (H&Y) stage were similar in DLB and PD-impaired groups. However, the severity of motor impairments on UPDRS was greater in DLB than in the PD-normal group (ANOVA, $F(2, 58) = 5.1$, $p = 0.01$; Tukey's post hoc t-test, $p = 0.01$). Visual hallucinations were common in DLB (prevalence 52.4%) and PD-impaired subjects (prevalence 31.3%) but were rare in PD-normal subjects (prevalence 4.2%; contrast of DLB vs. PD-normal, $\chi^2 = 13.3$, $p < 0.001$; contrast of PD-impaired vs PD-normal, $\chi^2 = 5.5$, $p = 0.02$).

When DLB and PD-impaired subjects were stratified by amyloid status (+/-), age, sex, and years of education were comparable across the four subgroups. Amyloid deposition was common in both DLB (fraction amyloid positive: 10/19) and PD-impaired subjects (7/16). The extent of deposition was similar in DLB compared to PD-impaired subjects (FLR DVR, DLB 1.68 ± 0.58, PD-impaired 1.30 ± 0.22, Mann-Whitney test, $p = 0.11$). In the PD-normal group, 6/24 had elevated PiB retention. Amyloid status did not impact cognitive impairment within diagnostic groups. Motor impairments and the prevalence of visual hallucinations were similar across all subgroups.

3.2. Patterns of cortical thinning

In DLB, vertex-based analyses demonstrated widespread cortical thinning ($p < 0.05$, FDR corrected), most severe in frontal, parietal, lateral and medial temporal regions (Fig. 1A). In the PD-impaired group, thinning was evident in an overlapping distribution ($p < 0.05$, FDR corrected) but spared medial temporal regions (Fig. 1B). The distribution of cortical thinning in the DLB and PD-impaired groups included AD signature regions (nine cortical ROIs), with additional involvement of precentral, paracentral, and fusiform regions (Fig. 2A; Table 2; Supplementary Table 1). No significant cortical thinning was observed in the PD-normal group.

Similar results were observed at the ROI level: both DLB and PD-impaired groups had marked cortical thinning in the AD signature regions taken as a whole, compared to PD-normal and HC groups (Fig. 2B, ANOVA, $F(3, 172) = 23.2$, $p = 1 \times 10^{-12}$; Tukey's post hoc t-test, $p < 0.005$). Compared to PD-normal and HC groups, both DLB and PD-impaired groups showed significant thinning in primary motor (aggregated precentral and paracentral) regions (Fig. 2C, ANOVA, $F(3, 172) = 14.1$, $p = 3 \times 10^{-8}$; Tukey's post hoc t-test, $p < 0.05$), as well as in the fusiform (Fig. 2D, ANOVA, $F(3, 172) = 22.3$, $p = 3 \times 10^{-12}$; Tukey's post hoc t-test, $p < 0.05$). No significant difference was observed in the extent of cortical thinning between DLB and PD-impaired groups in the AD signature, primary motor, or fusiform regions.

Cortical thinning in DLB was greatest in the medial temporal cortex with a mean magnitude of thinning of 0.39 mm (12% reduction compared to HC, ANOVA, $F(3, 172) = 9.5$, $p = 8 \times 10^{-6}$; Tukey's post hoc t-test, $p = 6 \times 10^{-5}$, Bonferroni corrected for number of ROIs). Other regions with more than 0.2 mm thinning included the precentral, fusiform, temporal pole, and inferior parietal (supramarginal) regions, which ranged from 8.8 – 10.5% thinner than HC (each comparison, Tukey's post hoc t-test, $p < 0.001$, Bonferroni corrected). A smaller magnitude of thinning (0.13–0.19 mm, 5.8–7.6%) was also observed in inferior temporal, precuneus, angular, paracentral, inferior frontal, superior frontal and superior parietal regions (Tukey's post hoc t-test, $p < 0.05$, Bonferroni corrected).

In the PD-impaired group, in contrast to DLB, cortical thickness in medial and inferior temporal regions was normal (ANOVA, for medial temporal cortex, $F(3, 172) = 9.5$, $p = 8 \times 10^{-6}$, for inferior temporal cortex, $F(3, 172) = 7.1$, $p = 2 \times 10^{-4}$; Tukey's post hoc t-test, for medial temporal cortex, $p = 0.36$, for inferior temporal cortex, $p = 0.09$). Cortical thinning in PD-impaired subjects was greatest in superior frontal cortex (0.22 mm, 8.4% reduction, ANOVA, $F(3, 172) = 12.9$, $p = 1 \times 10^{-7}$; Tukey's post hoc t-test, $p = 2 \times 10^{-4}$, Bonferroni corrected). Cortical thinning was also observed in the precentral (0.20 mm, 8.1%) and paracentral cortex (0.14 mm, 5.9%), fusiform (0.12 mm, 4.6%), precuneus (0.18 mm, 7.2%), superior parietal lobule (0.16 mm, 7.3%), and angular gyrus (0.15 mm, 6.2%) (all contrasts, Tukey's post hoc t-test, $p < 0.05$, Bonferroni corrected). The severity of cortical thinning was similar in the PD-impaired group and the DLB group in each of these regions, except for fusiform cortical thickness which was thinner in DLB compared to the PD-impaired group but did not survive multiple comparisons correction (ANOVA, $F(3, 172) = 22.3$, $p = 3 \times 10^{-12}$; Tukey's post hoc t-test, $p = 0.04$, Bonferroni uncorrected). As mentioned previously, the fusiform gyrus is not a consistent area of cortical thinning in AD. Interestingly, the three other areas with the most prominent thinning in DLB (medial temporal cortex, temporal pole, and supramarginal gyrus) are also consistently affected in AD and were much less affected in the PD-impaired group. Of note, when analyses were restricted to subjects with PDD, cortical thickness in the medial temporal cortex remained similar to HC (ANOVA, $F(3, 165) = 9.7$, $p = 6 \times 10^{-6}$; Tukey's post hoc t-test, $p = 0.42$).

Together, these results show that the DLB and PD-impaired groups shared a largely similar spatial pattern of cortical thinning that extended beyond the AD signature regions but differed with respect to temporal lobe involvement, with the DLB group having much more widespread medial, ventral, and ventrolateral temporal cortex thinning than the PD-impaired group.

3.3. The effect of amyloid accumulation on cortical thinning in LBD

In vertex-based analyses, DLB and PD-impaired subjects with high PiB retention (amyloid positive) showed more extensive and severe

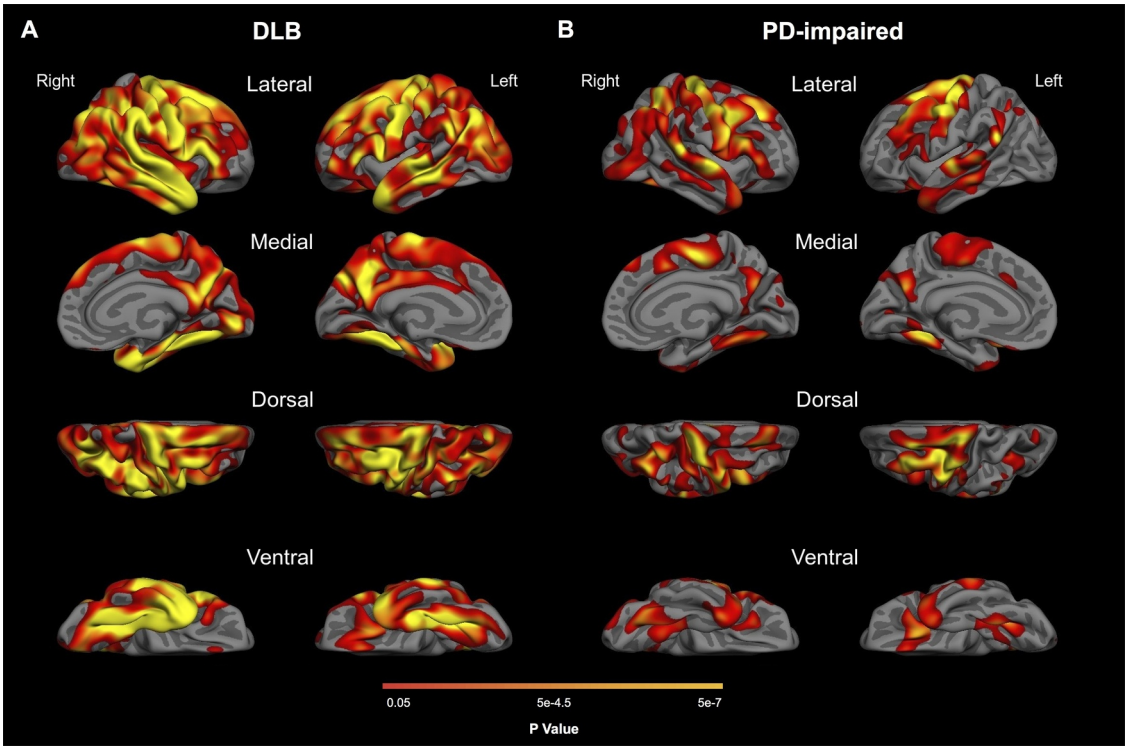

Fig. 1. Patterns of cortical thinning in DLB and PD-impaired groups. Maps show FDR-corrected ($p < 0.05$) results from general linear models comparing healthy controls with (A) DLB and (B) PD-impaired groups.

cortical thinning than subjects with low PiB retention (amyloid negative) (Fig. 3). The topography and extent of cortical thinning was broadly similar in amyloid-positive DLB and PD-impaired subjects, evident in both groups in frontal, parietal, and lateral temporal regions including AD-signature regions. However, as in the above analyses, the medial, ventral, and lateral temporal lobes showed a notably more widespread pattern of cortical thinning in amyloid-positive DLB than in the amyloid-positive PD-impaired group. In the amyloid-positive PD-impaired group, a relatively more prominent pattern of thinning in the dorsolateral prefrontal cortex was present, compared with DLB. The medial temporal cortex was spared in the PD-impaired group. In contrast, the pattern of cortical thinning evident in amyloid-negative DLB was much more restricted, with effects in dorsolateral prefrontal, precentral, and temporal cortex, but with much less lateral or medial parietal atrophy than in both amyloid-positive groups. Cortical thinning was not detected in amyloid-negative PD-impaired subjects. We were unable to detect an effect of amyloid deposition on cortical thickness in PD-normal patients in either vertex-based or ROI analyses. To confirm that the nonsignificant differences in age between groups did not contribute to these results or to the group contrasts independent of amyloid, we reran the analyses, contrasting the diagnostic groups with healthy control subjects tightly matched for age. After matching for mean and median age, the gamma maps remained essentially unchanged.

ROI-based analyses confirmed the vertex-based results. In ROI-based analyses of amyloid-positive DLB, the medial temporal lobe was most affected (0.44 mm, 13% thinning compared to HC), followed by the fusiform (0.36 mm, 13%), with additional cortical thinning in precentral, precuneus, supramarginal, angular, inferior frontal, and temporal polar regions (for each comparison: Tukey's post hoc test, $p < 0.05$, Bonferroni corrected for the number of ROIs; Table 3). In the amyloid-negative DLB subgroup, cortical thinning was less marked than in the amyloid-positive DLB subgroup. Interestingly, all but one ROI (the superior frontal gyrus) were slightly though not statistically thinner in the amyloid-positive DLB group than in the entire DLB group, whereas all but that same ROI were slightly though not statistically thicker in the amyloid-negative DLB group than in the entire DLB group. Considered with the more widespread spatial pattern of cortical thinning illustrated in the surface maps (Fig. 3), this suggests that cerebral amyloid is associated with greater cortical thinning in DLB. In ROI-based analyses of the amyloid-positive PD-impaired subgroup, the precentral region showed the greatest thinning (0.30 mm, 12% thinning), followed by the precuneus (0.21 mm, 12% thinning), with additional cortical thinning in superior frontal, paracentral, and angular regions (for each comparison: Tukey's post hoc test, $p < 0.05$, Bonferroni corrected). Cortical thinning was not evident at the ROI level in amyloid-negative PD-impaired subjects. Thus, in DLB and PD-impaired subjects but not in PD-normal subjects, amyloid deposition was associated with greater cortical thinning.

3.4. Regional cortical thinning relates to clinical features

In the DLB group, cortical thickness in the AD signature was negatively correlated with cognitive functional impairment as measured with the CDR-SB score (age adjusted partial Spearman rho $= -0.52$, $p = 0.02$) and was positively correlated with the MMSE score (partial Spearman rho $= 0.48$, $p = 0.03$; Fig. 4A,B). In the PD-impaired group, these findings were not observed (CDR-SB: partial Spearman rho $= -0.13$, $p = 0.65$), although a trend level correlation of moderate strength was observed between AD signature cortical thickness and the MMSE (partial Spearman rho $= 0.46$, $p = 0.09$). When the analyses were restricted to subjects with PDD, these correlations remained nonsignificant (CDR-SB: partial Spearman rho $= -0.41$, $p = 0.31$; MMSE: partial Spearman rho $= 0.17$, $p = 0.68$). In the PD-normal group, correlations between AD signature cortical thickness and CDR-SB and MMSE score were nonsignificant (CDR-SB: partial Spearman rho $= -0.04$, $p = 0.87$; MMSE: partial Spearman rho $= 0.15$, $p = 0.49$). When the correlations between cortical thinning in the AD signature and these cognitive functional measures were repeated in diagnostic subgroups stratified by amyloid status, only a trend level

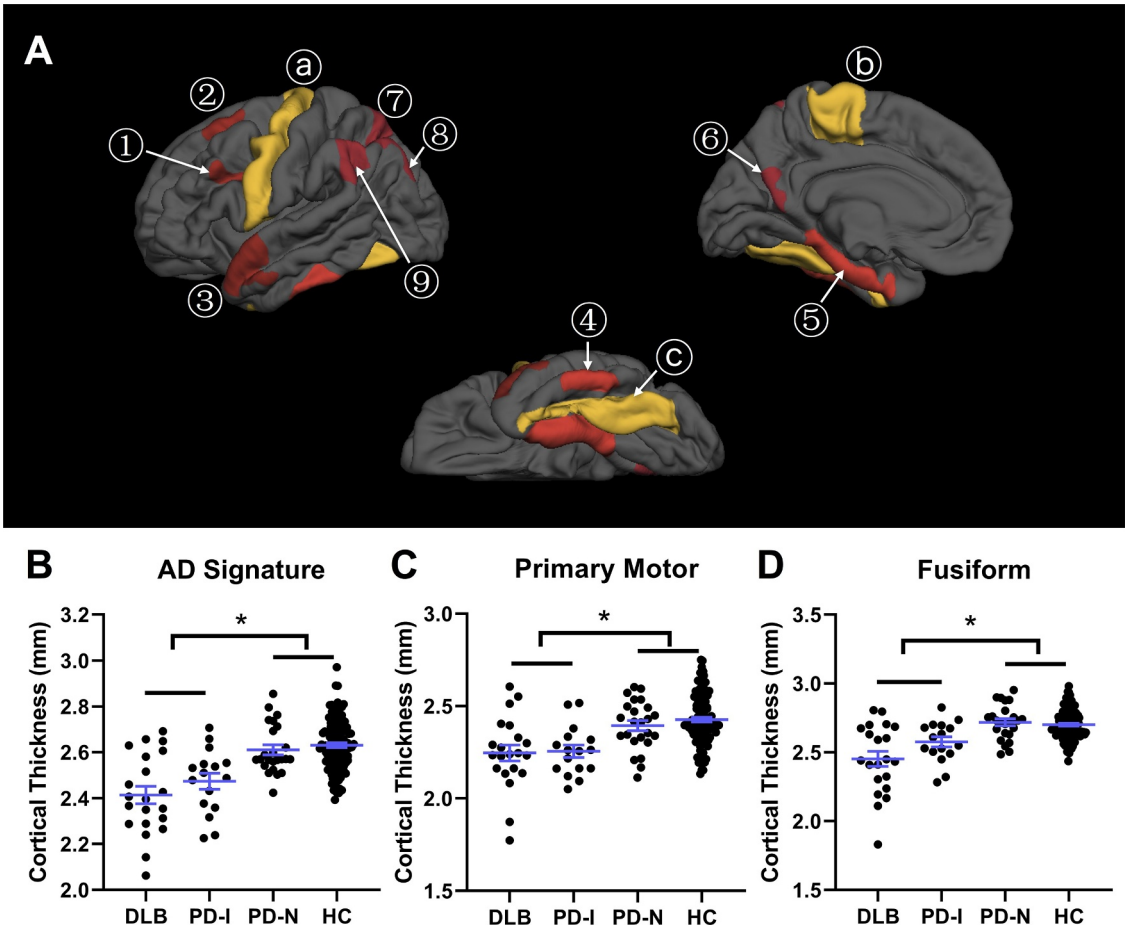

Fig. 2. Regional cortical thinning in LBD (A) Nine ROIs with characteristic thinning in AD derived from Dickerson et al. (2009) are shown in red, including ① inferior frontal sulcus, ② superior frontal gyrus, ③ temporal pole, ④ inferior temporal gyrus, ⑤ medial temporal cortex, ⑥ precuneus, ⑦ superior parietal lobule, ⑧ angular gyrus, and ⑨ supramarginal gyrus. Three additional regions, ⓐ precentral, ⓑ paracentral and ⓒ fusiform derived from the Desikan-Killiany atlas (Desikan et al., 2006) are shown in yellow. (B, C and D) Group comparisons of regional cortical thickness. Error bars (mean ± standard deviation) are displayed in blue. *, $p < 0.05$.

Table 2
Quantitative metrics of thinning by region .

ROIs	Mean thickness, mm (SD)				Mean difference			Percent thinning			Cohen d Effect Size		
	DLB	PD-I	PD-N	HC	DLB	PD-I	PD-N	DLB	PD-I	PD-N	DLB	PD-I	PD-N
MTL	2.96 (0.51)	3.21 (0.43)	3.36 (0.27)	3.35 (0.27)	0.39*	0.14	−0.01	11.68	4.21	0.29	1.24	0.49	0.04
IT	2.63 (0.27)	2.68 (0.24)	2.86 (0.16)	2.80 (0.19)	0.17*	0.12	−0.06	6.03	4.45	2.26	0.84	0.65	0.35
TP	2.67 (0.34)	2.77 (0.29)	3.02 (0.24)	2.98 (0.21)	0.31*	0.20 §	−0.05	10.53	6.86	1.54	1.34	0.94	0.22
AG	2.24 (0.19)	2.26 (0.15)	2.37 (0.15)	2.41 (0.15)	0.17*	0.15*	0.04	6.95	6.23	1.75	1.07	0.99	0.28
SFG	2.42 (0.25)	2.39 (0.19)	2.55 (0.18)	2.61 (0.15)	0.19*	0.22*	0.06	7.09	8.43	2.36	1.11	1.43	0.40
SPL	2.01 (0.17)	2.01 (0.19)	2.08 (0.14)	2.17 (0.15)	0.16*	0.16*	0.09	7.33	7.28	4.23	1.05	1.04	0.63
SMG	2.26 (0.22)	2.36 (0.15)	2.44 (0.19)	2.51 (0.17)	0.24*	0.15 §	0.06	9.72	5.80	2.58	1.36	0.87	0.37
Precuneus	2.35 (0.19)	2.36 (0.17)	2.55 (0.15)	2.54 (0.16)	0.19*	0.18*	−0.001	7.55	7.19	0.05	1.19	1.15	0.01
IFS	2.17 (0.13)	2.22 (0.10)	2.27 (0.14)	2.31 (0.12)	0.13*	0.09 §	0.04	5.79	3.79	1.85	1.11	0.75	0.35
FF	2.45 (0.25)	2.58 (0.15)	2.72 (0.13)	2.70 (0.11)	0.25*	0.12*	−0.02	9.18	4.62	0.66	1.78	1.10	0.16
PrC	2.26 (0.25)	2.28 (0.15)	2.43 (0.14)	2.48 (0.14)	0.22*	0.20*	0.04	8.82	8.12	1.76	1.40	1.48	0.32
ParC	2.23 (0.19)	2.24 (0.14)	2.36 (0.14)	2.38 (0.15)	0.14*	0.14*	0.02	5.99	5.90	0.88	0.92	0.96	0.14

Values represent mean (standard deviation) unless otherwise noted. For each ROI, average cortical thickness in disease groups was contrasted with healthy controls by ANOVA, following by Tukey's post hoc tests. Abbreviations: AG, Angular gyrus; DLB, Dementia with Lewy bodies; FF, Fusiform; IFS, Inferior frontal sulcus; IT, Inferior temporal gyrus; MTL, Medial temporal lobe; SFG, Superior frontal gyrus; SMG, Supramarginal gyrus; SPL, Superior parietal lobule; TP, Temporal pole; PD, Parkinson disease; PrC, Precentral; ParC, Paracentral.

* Disease group vs. healthy controls, $p < 0.05$, Bonferroni corrected for the number of ROIs.

§ Disease group vs. healthy controls, $p < 0.05$, uncorrected. These exploratory results did not survive after controlling for multiple comparisons.

correlation of moderate strength was observed for amyloid-negative DLB between AD signature thickness and CDR-SB score (for CDR-SB, amyloid-negative DLB: partial Spearman rho = −0.62, $p = 0.10$; amyloid-positive DLB: partial Spearman rho = −0.12, $p = 0.76$; amyloid-negative PD-impaired: partial Spearman rho = 0.25, $p = 0.55$; amyloid-positive PD-impaired: partial Spearman rho = −0.50, $p = 0.31$; for MMSE, amyloid-negative DLB: partial Spearman rho = 0.29, $p = 0.49$; amyloid-positive DLB: partial Spearman rho = 0.44, $p = 0.23$; amyloid-negative PD-impaired: partial Spearman rho = 0.33, $p = 0.43$; amyloid-positive PD-impaired: partial Spearman

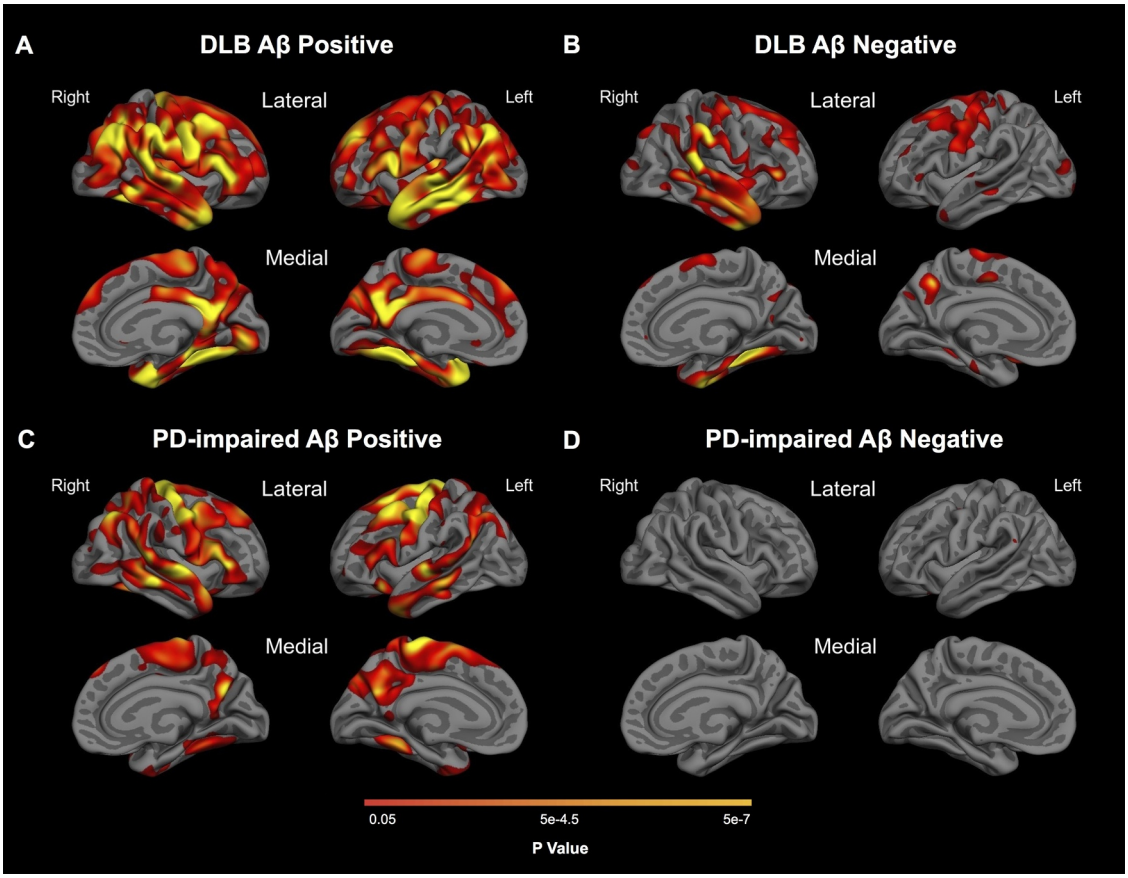

Fig. 3. Effect of amyloid deposition on cortical thinning in LBD. Maps show FDR-corrected ($p < 0.05$) results from general linear models comparing healthy controls with (A) amyloid-positive DLB, (B) amyloid-negative DLB, (C) amyloid-positive PD-impaired and (D) amyloid-negative PD-impaired groups.

rho = 0.36, $p = 0.49$).

Because the fusiform region has been implicated in higher order visual processing and expertise (Duchaine and Yovel, 2015), we next assessed whether fusiform cortical thickness also correlated with cognitive function. Similar to the above findings in AD-signature regions, fusiform cortical thickness correlated with cognitive impairment in DLB (CDR-SB score, age adjusted partial Spearman rho = −0.56, $p = 0.01$; MMSE score, partial Spearman rho = 0.57, $p = 0.01$; Fig. 4C,D). This correlation was not evident in the PD-impaired (CDR-SB score, partial Spearman rho = −0.28, $p = 0.30$; MMSE score, partial Spearman rho = 0.39, $p = 0.15$) or the PD-normal groups (CDR-SB score, partial Spearman rho = 0.11, $p = 0.63$; MMSE score, partial Spearman rho = −0.11, $p = 0.63$). Because visual hallucinations are common in the LBD, we also explored the possibility that fusiform cortical thickness might relate to the presence of visual hallucinations. However, DLB and PD-impaired diagnostic groups dichotomized on the basis of

Table 3
Quantitative metrics of thinning in subgroups stratified by amyloid status .

ROIs	Mean Thickness, mm (SD)				Mean difference				Percent thinning				Cohen d Effect Size			
	DLB		PD-impaired		DLB		PD-impaired		DLB		PD-impaired		DLB		PD-impaired	
Aβ Status	+	−	+	−	+	−	+	−	+	−	+	−	+	−	+	−
ADsig	2.38 (0.18)	2.43 (0.18)	2.41 (0.11)	2.53 (0.15)	0.25*	0.20*	0.22*	0.11	9.45	7.48	8.51	4.00	2.07	1.65	1.98	0.91
MTL	2.92 (0.67)	2.97 (0.37)	3.07 (0.42)	3.33 (0.43)	0.44*	0.39	0.29	0.03	13.06	11.52	8.53	0.86	1.39	1.40	1.03	0.10
IT	2.60 (0.18)	2.63 (0.33)	2.66 (0.21)	2.69 (0.26)	0.20	0.17	0.14	0.11	6.97	6.11	5.16	3.89	1.05	0.86	0.77	0.57
TP	2.61 (0.33)	2.70 (0.37)	2.70 (0.36)	2.83 (0.21)	0.37*	0.28	0.28	0.15	12.38	9.38	9.28	4.98	1.68	1.25	1.27	0.71
AG	2.18 (0.16)	2.28 (0.19)	2.17 (0.07)	2.33 (0.15)	0.23*	0.13	0.24*	0.08	9.53	5.35	10.05	3.27	1.70	0.92	1.17	0.62
SFG	2.46 (0.27)	2.37 (0.23)	2.34 (0.23)	2.43 (0.17)	0.15	0.24*	0.27*	0.18	5.70	9.26	10.25	7.01	0.93	1.56	1.75	1.22
SPL	2.00 (0.18)	2.02 (0.19)	1.95 (0.06)	2.06 (0.24)	0.17	0.15	0.21	0.11	7.87	6.80	9.91	5.24	1.14	0.98	1.50	0.73
SMG	2.21 (0.21)	2.35 (0.23)	2.31 (0.11)	2.40 (0.16)	0.29*	0.16	0.20	0.10	11.77	6.40	7.88	4.18	1.70	0.92	1.17	0.62
Precuneus	2.31 (0.17)	2.40 (0.22)	2.25 (0.14)	2.45 (0.15)	0.23*	0.15	0.21*	0.11	9.18	5.66	11.60	3.76	1.48	0.89	1.90	0.61
IFS	2.15 (0.09)	2.20 (0.16)	2.22 (0.09)	2.22 (0.11)	0.16*	0.11	0.09	0.08	6.82	4.83	3.94	3.68	1.34	0.91	0.77	0.72
FF	2.34 (0.26)	2.55 (0.22)	2.53 (0.15)	2.61 (0.14)	0.36*	0.15	0.17	0.09	13.18	5.68	6.30	3.31	2.83	1.29	1.54	0.81
PrC	2.25 (0.24)	2.28 (0.29)	2.18 (0.12)	2.35 (0.13)	0.23*	0.20*	0.30*	0.13	9.22	7.93	11.88	5.20	1.57	1.31	2.19	0.96
ParC	2.21 (0.15)	2.25 (0.25)	2.15 (0.06)	2.31 (0.15)	0.16	0.12	0.23*	0.07	10.19	8.03	4.04	4.98	1.10	0.79	1.58	0.48

Values represent mean (standard deviation) unless otherwise noted. For each ROI, average cortical thickness was contrasted in disease groups with healthy controls by ANOVA, following by Tukey's post hoc tests. Abbreviations: AG, Angular gyrus; DLB, Dementia with Lewy bodies; FF, Fusiform; IFS, Inferior frontal sulcus; IT, Inferior temporal gyrus; MTL, Medial temporal lobe; ParC, Paracentral; PrC, Precentral; PD, Parkinson disease; SFG, Superior frontal gyrus; SMG, Supramarginal gyrus; SPL, Superior parietal lobule; TP, Temporal pole.

* Disease group vs. healthy controls, $p < 0.05$, Bonferroni corrected for the number of ROIs.

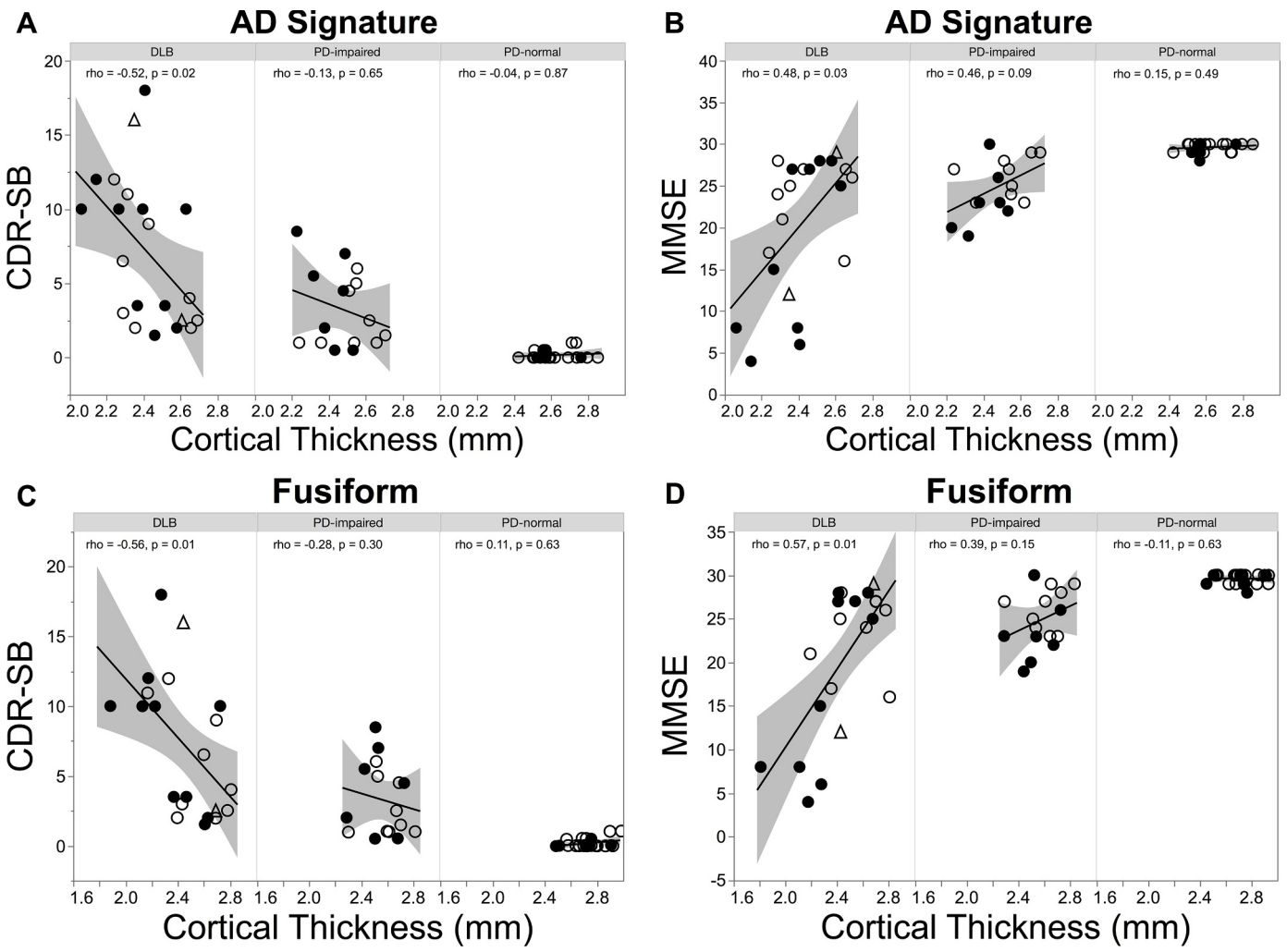

Fig. 4. Regional cortical thinning in LBD correlates with clinical features. Scatter plots between (A) AD signature cortical thickness and CDR-SB score, (B) AD signature cortical thickness and MMSE score, (C) fusiform cortical thickness and CDR-SB score, and (D) fusiform cortical thickness and MMSE score. Correlation coefficients rho and p values adjusted by age are shown. Filled circles, amyloid-positive status; open circles, amyloid-negative status; triangles, unknown amyloid status. .

visual hallucinations did not differ in their fusiform cortical thickness (DLB with hallucinations 2.44 ± 0.26, DLB without hallucinations 2.39 ± 0.30, two-tailed *t*-test, $p = 0.94$; PD-impaired with hallucinations 2.55 ± 0.16, PD-impaired without hallucinations 2.60 ± 0.15, two-tailed *t*-test, $p = 0.72$). These results persisted in contrasts of DLB and PD-impaired subgroups stratified by amyloid status: For both amyloid positive and amyloid negative diagnostic subgroups, the presence of hallucinations did not affect fusiform cortical thickness (for each diagnostic subgroup of each amyloid status, two-tailed *t*-test, $p > 0.51$).

Given that thinning in primary motor cortical regions was a prominent finding in DLB and PD-impaired groups, we next evaluated its relation to motor impairment. Within each diagnostic group, primary motor cortical thickness was not significantly correlated with UPDRS motor scores (DLB: partial Spearman rho $= -0.04$, $p = 0.86$; PD-impaired: rho $= -0.14$, $p = 0.62$; PD-normal: rho $= -0.21$, $p = 0.33$). To determine whether amyloid deposition impacted this relationship, we repeated these analyses after stratifying by amyloid status. In the amyloid-negative DLB subgroup alone, greater thinning in primary motor cortex was associated with greater impairment on the UPDRS (amyloid-negative DLB: partial Spearman rho $= -0.75$, $p = 0.03$; amyloid-positive DLB: partial Spearman rho $= 0.38$, $p = 0.32$; amyloid-negative PD-impaired: partial Spearman rho $= -0.27$, $p = 0.52$; amyloid-positive PD-impaired: partial Spearman rho $= 0.35$, $p = 0.50$; Supplemental Figure 1).

Together, these observations suggest that cortical thinning in AD signature and fusiform regions contributes to cognitive impairment in the LBD and raise the possibility that thinning in primary motor regions may contribute to motor impairment in DLB.

4. Discussion

The results of this study identify a pattern of cortical thinning shared between DLB and PD-impaired groups. The distribution of thinning overlapped with AD signature regions and extended to involve fusiform, precentral and paracentral cortex. In prior voxel-based morphometry studies, patterns of cortical atrophy in DLB and PDD have also been found to overlap (Burton et al., 2004), albeit with greater volume loss in DLB (Beyer et al., 2007; Sanchez-Castaneda et al., 2009; Song et al., 2011; Summerfield et al., 2005; Weintraub et al., 2011). Our results are also consistent with studies that have evaluated cortical thickness in DLB (Lee et al., 2018; Watson et al., 2015) and extend these findings to PD-associated cognitive impairment. The observation of thinning in primary motor cortices in the Lewy body diseases is interesting in light of the motor impairments that arise in these diseases. This finding is consistent with a neuropathological report showing that Lewy body pathology is associated with precentral cortical atrophy (Harper et al., 2017).

In DLB, amyloid deposition was associated with markedly accentuated thinning that was widely distributed across many cortical regions, including the medial temporal lobe, consistent with recent reports (Lee et al., 2018; Mak et al., 2019; van der Zande et al., 2018). In the absence of amyloid, cortical thinning in DLB could still be detected, revealing a synuclein-dependent pattern of cortical thinning that overlapped with and extended beyond the AD signature to include the precentral cortex, among other regions. However, medial temporal cortical thinning, a characteristic feature of AD, was much less prominent in DLB without amyloid than in DLB in the presence of cortical amyloid.

The impact of cortical amyloid in PD-impaired subjects was similar to DLB but distinct, driving distributed cortical thinning that spared the medial temporal cortex. The basis for this distinction is unclear but may relate to the nonsignificantly lower amyloid burden observed in the PD-impaired group compared to the DLB group. Differences between the groups in the level of cognitive impairment is unlikely to be explanatory, given that medial temporal sparing persisted when PDD subjects with comparable cognitive impairment were evaluated. Interestingly, amyloid deposition explained the full extent of cortical thinning detected in PD-impaired subjects: cortical thinning was not observed in PD-impaired participants with low amyloid burden. This result builds on previous studies of PDD (Compta et al., 2012; Mak et al., 2017), where CSF markers of AD pathology have been found to correlate with gray matter atrophy and where AD co-pathology at autopsy has been associated with more severe and more widely distributed cortical atrophy (de la Monte et al., 1989).

In contrast to DLB and PD-impaired participants, amyloid deposition did not influence cortical thickness in cognitively normal PD participants. This result suggests that amyloid alone is not responsible for thinning and cognitive impairment, but instead works in concert with other molecular pathologies, including but not limited to neuromodulator loss (Gomperts, 2014; Halliday et al., 2014), cortical alpha-synuclein aggregates (Calo et al., 2016; Colom-Cadena et al., 2017; Schulz-Schaeffer, 2010), and tau deposits (Gomperts et al., 2016; Hansen et al., 2017) that are necessary for the neuropathological cascades that underlie atrophy and accelerate cognitive impairment (Gomperts et al., 2013; Siderowf et al., 2010) in the LBD. In this regard, neurofibrillary tangles measured with tau PET have been shown to correlate with cognitive impairment (Gomperts et al., 2016; Smith et al., 2018).

With respect to the clinical repercussions of cortical thinning, consistent with previous studies (Elder et al., 2017; Sanchez-Castaneda et al., 2009), we observed a strong association in DLB between greater cortical thinning in AD signature regions and greater cognitive functional impairment. Although we found only a trend-level relation in PD-impaired subjects, we anticipate that differences in the extent of cortical thinning and in the severity of cognitive impairment in the DLB and PD-impaired groups may have contributed to this apparent distinction. Similar findings were found for the fusiform region implicated in higher order visual processing (Duchaine and Yovel, 2015), where greater thinning was associated with greater cognitive impairment in DLB. Together, these results suggest that thinning in both AD signature regions and the fusiform cortex contribute to cognitive impairment in the LBD.

In contrast to the impact of regional cortical thinning on cognitive function, we did not detect a significant association between the extent of precentral and paracentral cortical thinning and the severity of motor impairment in any Lewy body disease group. After stratification on the basis of amyloid status, however, such a relationship was evident in amyloid-negative DLB subjects. Due to limited sample sizes in amyloid-stratified subgroups, we consider this result exploratory, but we note that it supports the possibility that the disparate molecular cascades that contribute to cortical thinning in the LBD (synuclein-dependent and amyloid-dependent cascades differentially manifesting in synapse loss, cell death of distinct populations, or other causes of loss of neuropil) may have distinct repercussions on clinical function.

Strengths of this study include the inclusion of clinically well-characterized participants with both DLB and PD across a range of cognitive impairment, including PD-MCI and PDD. The use of Freesurfer permitted high resolution cortical thickness measurements that build on prior volume based approaches. In addition, the stratification of cortical thickness on the basis of amyloid burden has, to our knowledge, never been applied to PD or to its contrast with DLB. However, there are also some limitations. Because healthy control subjects did not undergo amyloid imaging, some controls were likely amyloid positive. This may have reduced our sensitivity to detect differences between the diagnostic groups and the healthy controls. In support of the high specificity of the clinical criteria used to diagnose Lewy body disease, as shown previously (Huang and Halliday, 2013; Nelson et al., 2010), all 18 LBD subjects who underwent neuropathologic assessment had Lewy body disease. In addition, the greater cognitive and motor impairments of the DLB group compared to the PD-impaired group may have contributed to the apparent differences between these groups. However, analyses restricted to PDD subjects gave similar results to those of the PD-impaired group. The diagnostic groups were well-matched for age, and the results of the vertex-based analyses were unchanged after tight matching for age across the groups. Even so, future vertex-wide analyses with larger datasets using age as a covariate will be useful to exclude the possible contribution of group differences in age-related atrophy. Another possible weakness is the small sample sizes of subgroups stratified by amyloid, but the impact of amyloid on cortical thinning was evident in any case. We conclude that the topography of cortical thinning is broadly similar in DLB and PD-associated impairment, is markedly influenced by amyloid deposition, and impacts cognitive function.

CRediT authorship contribution statement

Rong Ye: Data curation, Formal analysis, Investigation, Methodology, Project administration, Software, Validation, Visualization, Writing - original draft, Writing - review & editing. **Alexandra Touroutoglou:** Formal analysis, Investigation, Methodology, Project administration, Software, Validation, Visualization, Writing - original draft, Writing - review & editing. **Michael Brickhouse:** Data curation, Methodology, Project administration, Software, Validation, Visualization. **Samantha Katz:** Data curation, Methodology, Project administration, Software, Validation, Visualization. **John H. Growdon:** Writing - review & editing. **Keith A. Johnson:** Methodology, Resources, Software. **Bradford C. Dickerson:** Conceptualization, Funding acquisition, Investigation, Methodology, Resources, Supervision, Writing - original draft, Writing - review & editing. **Stephen N. Gomperts:** Conceptualization, Funding acquisition, Investigation, Methodology, Resources, Supervision, Writing - original draft, Writing - review & editing.

Declaration of Competing Interest

Dr.. Rong Ye reports no disclosures.

Dr.. Alexandra Touroutoglou reports no disclosures.

Mr. Michael Brickhouse reports no disclosures.

Ms. Samantha Katz reports no disclosures.

Dr.. John Growdon reports support from NIA and Advisory Board Neuroimmune Holding.

Dr.. Keith A. Johnson has served as a paid consultant for Bayer, GE Healthcare, Janssen Alzheimer's Immunotherapy, Siemens Medical Solutions, Genzyme, Novartis, Biogen, Roche, ISIS Pharma, AZTherapy, GEHC, Lundberg, and Abbvie. He is a site coinvestigator for Lilly/Avid, Pfizer, Janssen Immunotherapy, and Navidea. He has spoken at symposia sponsored by Janssen Alzheimer's Immunotherapy and Pfizer. He receives funding from NIH grants R01EB014894, R21 AG038994, R01 AG026484, R01 AG034556, P50 AG00513421, U19 AG10483, P01 AG036694, R13 AG042201174210, R01 AG027435, and R01

AG037497 and the Alzheimer's Association grant ZEN-10–174,210.

Dr.. Bradford C. Dickerson has served as a paid consultant for Novartis, Avexis, Biogen, Lilly, Wave LifeSciences, Merck, and Arkuda. He receives royalties from Oxford University Press and Cambridge University Press. He receives funding from NIH grants P01 AG036694, R01 AG045390, R01 AG038791, R01 AG048351, R01 DC014296, U01 AG052943, R01 AG056015, R21 AG056958, R01 AG054081, R01MH112737, R01MH109464, R01MH113234, R56AG058745, U01AG057195, R01 AG0061968, P01 AG031720, P30AG062421 and the Alzheimer's Drug Discovery Foundation and the ALS Association.

Dr.. Stephen N. Gomperts has served on Advisory Boards for Acadia Pharmaceuticals and Sanofi. He receives funding from NIH grant R01 AG054551, R01 AG062208, P50 AG005134, R21 NS109833, DOD CDMRP/W81XW1810516, the Farmer Family Parkinson's Initiative, and the Lewy Body Dementia Association.

Acknowledgements

The authors thank Larissa Werneck (MGH, Department of Neurology) for research assistance. Research reported in this publication was supported by the Department of Defense CDMRP/W81XW1810516 and the Lewy Body Dementia Association and NIH grant P30AG062421.

Supplementary materials

Supplementary material associated with this article can be found, in the online version, at doi:10.1016/j.nicl.2020.102196.

References

Bakkour, A., Morris, J.C., Dickerson, B.C., 2009. The cortical signature of prodromal AD: regional thinning predicts mild AD dementia. Neurology 72, 1048–1055.

Bakkour, A., Morris, J.C., Wolk, D.A., Dickerson, B.C., 2013. The effects of aging and Alzheimer's disease on cerebral cortical anatomy: specificity and differential relationships with cognition. Neuroimage 76, 332–344.

Beekly, D.L., Ramos, E.M., Lee, W.W., Deitrich, W.D., Jacka, M.E., Wu, J., Hubbard, J.L., Koepsell, T.D., Morris, J.C., Kukull, W.A., Centers, N.I.A.A.s.D., 2007. The national Alzheimer's coordinating center (NACC) database: the uniform data set. Alzheimer Dis Assoc Disord 21, 249–258.

Beyer, M.K., Larsen, J.P., Aarsland, D., 2007. Gray matter atrophy in parkinson disease with dementia and dementia with Lewy bodies. Neurology 69, 747–754.

Bickart, K.C., Brickhouse, M., Negreira, A., Sapolsky, D., Barrett, L.F., Dickerson, B.C., 2014. Atrophy in distinct corticolimbic networks in frontotemporal dementia relates to social impairments measured using the social impairment rating scale. J Neurol Neurosurg Psychiatry 85, 438–448.

Borroni, B., Premi, E., Formenti, A., Turrone, R., Alberici, A., Cottini, E., Rizzetti, C., Gasparotti, R., Padovani, A., 2015. Structural and functional imaging study in dementia with Lewy bodies and Parkinson's disease dementia. Parkinsonism Relat Disord 21, 1049–1055.

Burton, E.J., McKeith, I.G., Burn, D.J., Williams, E.D., O'Brien, J.T., 2004. Cerebral atrophy in Parkinson's disease with and without dementia: a comparison with Alzheimer's disease, dementia with Lewy bodies and controls. Brain 127, 791–800.

Calo, L., Wegrzynowicz, M., Santivanez-Perez, J., Grazia Spillantini, M., 2016. Synaptic failure and alpha-synuclein. Mov Disord 31, 169–177.

Colom-Cadena, M., Pegueroles, J., Herrmann, A.G., Henstridge, C.M., Munoz, L., Querol-Vilaseca, M., Martin-Paniello, C.S., Luque-Cabecerans, J., Clarimon, J., Belbin, O., Nunez-Llaves, R., Blesa, R., Smith, C., McKenzie, C.A., Frosch, M.P., Roe, A., Fortea, J., Andilla, J., Loza-Alvarez, P., Gelpi, E., Hyman, B.T., Spires-Jones, T.L., Lleo, A., 2017. Synaptic phosphorylated alpha-synuclein in dementia with Lewy bodies. Brain 140, 3204–3214.

Compta, Y., Ibarretxe-Bilbao, N., Pereira, J.B., Junque, C., Bargallo, N., Tolosa, E., Valldeoriola, F., Munoz, E., Camara, A., Buongiorno, M., Marti, M.J., 2012. Grey matter volume correlates of cerebrospinal markers of Alzheimer-pathology in Parkinson's disease and related dementia. Parkinsonism Relat Disord 18, 941–947.

de la Monte, S.M., Wells, S.E., Hedley-Whyte, T., Growdon, J.H., 1989. Neuropathological distinction between Parkinson's dementia and Parkinson's plus Alzheimer's disease. Ann Neurol 26, 309–320.

Desikan, R.S., Segonne, F., Fischl, B., Quinn, B.T., Dickerson, B.C., Blacker, D., Buckner, R.L., Dale, A.M., Maguire, R.P., Hyman, B.T., Albert, M.S., Killiany, R.J., 2006. An automated labeling system for subdividing the human cerebral cortex on MRI scans into gyral based regions of interest. Neuroimage 31, 968–980.

Dickerson, B.C., Bakkour, A., Salat, D.H., Feczko, E., Pacheco, J., Greve, D.N., Grodstein, F., Wright, C.I., Blacker, D., Rosas, H.D., Sperling, R.A., Atri, A., Growdon, J.H., Hyman, B.T., Morris, J.C., Fischl, B., Buckner, R.L., 2009. The cortical signature of Alzheimer's disease: regionally specific cortical thinning relates to symptom severity in very mild to mild AD dementia and is detectable in asymptomatic amyloid-positive individuals. Cereb Cortex 19, 497–510.

Dickerson, B.C., Stoub, T.R., Shah, R.C., Sperling, R.A., Killiany, R.J., Albert, M.S., Hyman, B.T., Blacker, D., Detoledo-Morrell, L., 2011. Alzheimer-signature MRI biomarker predicts AD dementia in cognitively normal adults. Neurology 76, 1395–1402.

Duchaine, B., Yovel, G., 2015. A revised neural framework for face processing. Annu Rev Vis Sci 1, 393–416.

Elder, G.J., Mactier, K., Colloby, S.J., Watson, R., Blamire, A.M., O'Brien, J.T., Taylor, J.P., 2017. The influence of hippocampal atrophy on the cognitive phenotype of dementia with Lewy bodies. Int J Geriatr Psychiatry 32, 1182–1189.

Emre, M., Aarsland, D., Brown, R., Burn, D.J., Duyckaerts, C., Mizuno, Y., Broe, G.A., Cummings, J., Dickson, D.W., Gauthier, S., Goldman, J., Goetz, C., Korczyn, A., Lees, A., Levy, R., Litvan, I., McKeith, I., Olanow, W., Poewe, W., Quinn, N., Sampaio, C., Tolosa, E., Dubois, B., 2007. Clinical diagnostic criteria for dementia associated with Parkinson's disease. Mov Disord 22, 1689–1707 quiz 1837.

Ferman, T.J., Smith, G.E., Boeve, B.F., Ivnik, R.J., Petersen, R.C., Knopman, D., Graff-Radford, N., Parisi, J., Dickson, D.W., 2004. DLB fluctuations: specific features that reliably differentiate DLB from AD and normal aging. Neurology 62, 181–187.

Fischl, B., Dale, A.M., 2000. Measuring the thickness of the human cerebral cortex from magnetic resonance images. Proc Natl Acad Sci U S A 97, 11050–11055.

Fischl, B., Sereno, M.I., Dale, A.M., 1999. Cortical surface-based analysis. II: inflation, flattening, and a surface-based coordinate system. Neuroimage 9, 195–207.

Gomperts, S.N., 2014. Imaging the role of amyloid in PD dementia and dementia with Lewy bodies. Curr Neurol Neurosci Rep 14, 472.

Gomperts, S.N., Locascio, J.J., Makaretz, S.J., Schultz, A., Caso, C., Vasdev, N., Sperling, R., Growdon, J.H., Dickerson, B.C., Johnson, K., 2016. Tau positron emission tomographic imaging in the Lewy body diseases. JAMA Neurol 73, 1334–1341.

Gomperts, S.N., Locascio, J.J., Rentz, D., Santarlasci, A., Marquie, M., Johnson, K.A., Growdon, J.H., 2013. Amyloid is linked to cognitive decline in patients with Parkinson disease without dementia. Neurology 80, 85–91.

Greve, D.N., Salat, D.H., Bowen, S.L., Izquierdo-Garcia, D., Schultz, A.P., Catana, C., Becker, J.A., Svarer, C., Knudsen, G.M., Sperling, R.A., Johnson, K.A., 2016. Different partial volume correction methods lead to different conclusions: an (18)F-FDG-PET study of aging. Neuroimage 132, 334–343.

Halliday, G.M., Leverenz, J.B., Schneider, J.S., Adler, C.H., 2014. The neurobiological basis of cognitive impairment in Parkinson's disease. Mov Disord 29, 634–650.

Hansen, A.K., Damholdt, M.F., Fedorova, T.D., Knudsen, K., Parbo, P., Ismail, R., Ostergaard, K., Brooks, D.J., Borghammer, P., 2017. In vivo cortical tau in Parkinson's disease using 18F-AV-1451 positron emission tomography. Mov Disord 32, 922–927.

Harding, A.J., Halliday, G.M., 2001. Cortical Lewy body pathology in the diagnosis of dementia. Acta Neuropathol 102, 355–363.

Harper, L., Bouwman, F., Burton, E.J., Barkhof, F., Scheltens, P., O'Brien, J.T., Fox, N.C., Ridgway, G.R., Schott, J.M., 2017. Patterns of atrophy in pathologically confirmed dementias: a voxelwise analysis. J Neurol Neurosurg Psychiatry 88, 908–916.

Huang, Y., Halliday, G., 2013. Can we clinically diagnose dementia with Lewy bodies yet? Transl Neurodegener 2, 4.

Hughes, A.J., Daniel, S.E., Blankson, S., Lees, A.J., 1993. A clinicopathologic study of 100 cases of Parkinson's disease. Arch Neurol 50, 140–148.

Hyman, B.T., Phelps, C.H., Beach, T.G., Bigio, E.H., Cairns, N.J., Carrillo, M.C., Dickson, D.W., Duyckaerts, C., Frosch, M.P., Masliah, E., Mirra, S.S., Nelson, P.T., Schneider, J.A., Thal, D.R., Thies, B., Trojanowski, J.Q., Vinters, H.V., Montine, T.J., 2012. National institute on aging-alzheimer's association guidelines for the neuropathologic assessment of Alzheimer's disease. Alzheimers Dement 8, 1–13.

Kang, S.W., Jeon, S., Yoo, H.S., Chung, S.J., Lee, P.H., Sohn, Y.H., Yun, M., Evans, A.C., Ye, B.S., 2019. Effects of Lewy body disease and Alzheimer disease on brain atrophy and cognitive dysfunction. Neurology 92, e2015–e2026.

Kuperberg, G.R., Broome, M.R., McGuire, P.K., David, A.S., Eddy, M., Ozawa, F., Goff, D., West, W.C., Williams, S.C., van der Kouwe, A.J., Salat, D.H., Dale, A.M., Fischl, B., 2003. Regionally localized thinning of the cerebral cortex in schizophrenia. Arch Gen Psychiatry 60, 878–888.

Lee, J.E., Park, B., Song, S.K., Sohn, Y.H., Park, H.J., Lee, P.H., 2010. A comparison of gray and white matter density in patients with Parkinson's disease dementia and dementia with Lewy bodies using voxel-based morphometry. Mov Disord 25, 28–34.

Lee, Y.G., Jeon, S., Yoo, H.S., Chung, S.J., Lee, S.K., Lee, P.H., Sohn, Y.H., Yun, M., Evans, A.C., Ye, B.S., 2018. Amyloid-beta-related and unrelated cortical thinning in dementia with Lewy bodies. Neurobiol Aging 72, 32–39.

Litvan, I., Goldman, J.G., Troster, A.I., Schmand, B.A., Weintraub, D., Petersen, R.C., Mollenhauer, B., Adler, C.H., Marder, K., Williams-Gray, C.H., Aarsland, D., Kulisevsky, J., Rodriguez-Oroz, M.C., Burn, D.J., Barker, R.A., Emre, M., 2012. Diagnostic criteria for mild cognitive impairment in Parkinson's disease: movement disorder society task force guidelines. Mov Disord 27, 349–356.

Mak, E., Donaghy, P.C., McKiernan, E., Firbank, M.J., Lloyd, J., Petrides, G.S., Thomas, A.J., O'Brien, J.T., 2019. Beta amyloid deposition maps onto hippocampal and subiculum atrophy in dementia with Lewy bodies. Neurobiol Aging 73, 74–81.

Mak, E., Su, L., Williams, G.B., Firbank, M.J., Lawson, R.A., Yarnall, A.J., Duncan, G.W., Mollenhauer, B., Owen, A.M., Khoo, T.K., Brooks, D.J., Rowe, J.B., Barker, R.A., Burn, D.J., O'Brien, J.T., 2017. Longitudinal whole-brain atrophy and ventricular enlargement in nondemented Parkinson's disease. Neurobiol Aging 55, 78–90.

McKeith, I.G., Boeve, B.F., Dickson, D.W., Halliday, G., Taylor, J.P., Weintraub, D., Aarsland, D., Galvin, J., Attems, J., Ballard, C.G., Bayston, A., Beach, T.G., Blanc, F., Bohnen, N., Bonanni, L., Bras, J., Brundin, P., Burn, D., Chen-Plotkin, A., Duda, J.E., El-Agnaf, O., Feldman, H., Ferman, T.J., Ffytche, D., Fujishiro, H., Galasko, D., Goldman, J.G., Gomperts, S.N., Graff-Radford, N.R., Honig, L.S., Iranzo, A., Kantarci, K., Kaufer, D., Kukull, W., Lee, V.M.Y., Leverenz, J.B., Lewis, S., Lippa, C., Lunde, A., Masellis, M., Masliah, E., McLean, P., Mollenhauer, B., Montine, T.J., Moreno, E.,

Mori, E., Murray, M., O'Brien, J.T., Orimo, S., Postuma, R.B., Ramaswamy, S., Ross, O.A., Salmon, D.P., Singleton, A., Taylor, A., Thomas, A., Tiraboschi, P., Toledo, J.B., Trojanowski, J.Q., Tsuang, D., Walker, Z., Yamada, M., Kosaka, K., 2017. Diagnosis and management of dementia with Lewy bodies: fourth consensus report of the DLB consortium. Neurology 89, 88–100.

Moriguchi, Y., Negreira, A., Weierich, M., Dautoff, R., Dickerson, B.C., Wright, C.I., Barrett, L.F., 2011. Differential hemodynamic response in affective circuitry with aging: an FMRI study of novelty, valence, and arousal. J Cogn Neurosci 23, 1027–1041.

Mormino, E.C., Betensky, R.A., Hedden, T., Schultz, A.P., Ward, A., Huijbers, W., Rentz, D.M., Johnson, K.A., Sperling, R.A., Alzheimer's disease neuroimaging, I., australian imaging, B., lifestyle flagship study of, A., harvard aging brain, S., 2014. Amyloid and APOE epsilon4 interact to influence short-term decline in preclinical Alzheimer disease. . Neurology 82, 1760–1767.

Morris, J.C., Weintraub, S., Chui, H.C., Cummings, J., Decarli, C., Ferris, S., Foster, N.L., Galasko, D., Graff-Radford, N., Peskind, E.R., Beekly, D., Ramos, E.M., Kukull, W.A., 2006. The uniform data set (UDS): clinical and cognitive variables and descriptive data from alzheimer disease centers. Alzheimer Dis Assoc Disord 20, 210–216.

Nelson, P.T., Jicha, G.A., Kryscio, R.J., Abner, E.L., Schmitt, F.A., Cooper, G., Xu, L.O., Smith, C.D., Markesbery, W.R., 2010. Low sensitivity in clinical diagnoses of dementia with Lewy bodies. J Neurol 257, 359–366.

Racine, A.M., Brickhouse, M., Wolk, D.A., Dickerson, B.C., Alzheimer's Disease Neuroimaging, I., 2018. The personalized Alzheimer's disease cortical thickness index predicts likely pathology and clinical progression in mild cognitive impairment. Alzheimers Dement (Amst) 10, 301–310.

Rosas, H.D., Liu, A.K., Hersch, S., Glessner, M., Ferrante, R.J., Salat, D.H., van der Kouwe, A., Jenkins, B.G., Dale, A.M., Fischl, B., 2002. Regional and progressive thinning of the cortical ribbon in Huntington's disease. Neurology 58, 695–701.

Salat, D.H., Buckner, R.L., Snyder, A.Z., Greve, D.N., Desikan, R.S., Busa, E., Morris, J.C., Dale, A.M., Fischl, B., 2004. Thinning of the cerebral cortex in aging. Cereb Cortex 14, 721–730.

Sanchez-Castaneda, C., Rene, R., Ramirez-Ruiz, B., Campdelacreu, J., Gascon, J., Falcon, C., Calopa, M., Jauma, S., Juncadella, M., Junque, C., 2009. Correlations between gray matter reductions and cognitive deficits in dementia with Lewy bodies and Parkinson's disease with dementia. Mov Disord 24, 1740–1746.

Sarro, L., Senjem, M.L., Lundt, E.S., Przybelski, S.A., Lesnick, T.G., Graff-Radford, J., Boeve, B.F., Lowe, V.J., Ferman, T.J., Knopman, D.S., Comi, G., Filippi, M., Petersen, R.C., Jack Jr., C.R., Kantarci, K., 2016. Amyloid-beta deposition and regional grey matter atrophy rates in dementia with Lewy bodies. Brain 139, 2740–2750.

Schulz-Schaeffer, W.J., 2010. The synaptic pathology of alpha-synuclein aggregation in dementia with Lewy bodies. Parkinson's disease and Parkinson's disease dementia. Acta Neuropathol 120, 131–143.

Shimada, H., Shinotoh, H., Hirano, S., Miyoshi, M., Sato, K., Tanaka, N., Ota, T., Fukushi, K., Irie, T., Ito, H., Higuchi, M., Kuwabara, S., Suhara, T., 2013. beta-Amyloid in Lewy body disease is related to Alzheimer's disease-like atrophy. Mov Disord 28, 169–175.

Siderowf, A., Xie, S.X., Hurtig, H., Weintraub, D., Duda, J., Chen-Plotkin, A., Shaw, L.M., Van Deerlin, V., Trojanowski, J.Q., Clark, C., 2010. CSF amyloid {beta} 1-42 predicts cognitive decline in parkinson disease. Neurology 75, 1055–1061.

Smith, R., Scholl, M., Londos, E., Ohlsson, T., Hansson, O., 2018. (18)F-AV-1451 in Parkinson's disease with and without dementia and in dementia with Lewy bodies. Sci Rep 8, 4717.

Song, S.K., Lee, J.E., Park, H.J., Sohn, Y.H., Lee, J.D., Lee, P.H., 2011. The pattern of cortical atrophy in patients with Parkinson's disease according to cognitive status. Mov Disord 26, 289–296.

Summerfield, C., Junque, C., Tolosa, E., Salgado-Pineda, P., Gomez-Anson, B., Marti, M.J., Pastor, P., Ramirez-Ruiz, B., Mercader, J., 2005. Structural brain changes in parkinson disease with dementia: a voxel-based morphometry study. Arch Neurol 62, 281–285.

van der Zande, J.J., Steenwijk, M.D., Ten Kate, M., Wattjes, M.P., Scheltens, P., Lemstra, A.W., 2018. Gray matter atrophy in dementia with Lewy bodies with and without concomitant Alzheimer's disease pathology. Neurobiol Aging 71, 171–178.

Watson, R., Colloby, S.J., Blamire, A.M., O'Brien, J.T., 2015. Assessment of regional gray matter loss in dementia with Lewy bodies: a surface-based MRI analysis. Am J Geriatr Psychiatry 23, 38–46.

Weintraub, D., Doshi, J., Koka, D., Davatzikos, C., Siderowf, A.D., Duda, J.E., Wolk, D.A., Moberg, P.J., Xie, S.X., Clark, C.M., 2011. Neurodegeneration across stages of cognitive decline in parkinson disease. Arch Neurol 68, 1562–1568.

APPENDIX – Manuscript published

HHS Public Access

Author manuscript

Parkinsonism Relat Disord. Author manuscript; available in PMC 2021 December 28.

Published in final edited form as:

Parkinsonism Relat Disord. 2021 April ; 85: 11–16. doi:10.1016/j.parkreldis.2021.02.008.

Serum NFL levels predict progression of motor impairment and reduction in putamen dopamine transporter binding ratios in de novo Parkinson's disease: An 8-year longitudinal study

Rong Ye[a,b], **Joseph J. Locascio**[b], **Anna E. Goodheart**[b], **Moqing Quan**[b], **Baorong Zhang**[a,**], **Stephen N. Gomperts**[b,*]

[a]Department of Neurology, Second Affiliated Hospital of School of Medicine, Zhejiang University, Hangzhou, China

[b]Department of Neurology, Massachusetts General Hospital, Boston, USA

Abstract

Neurofilament light chain (NFL) level in biofluids is a sensitive measure of axonal damage and a promising biomarker in neurodegenerative diseases. In Parkinson's disease (PD), NFL can distinguish PD from other parkinsonian disorders, and NFL concentration is associated with disease severity, risk of progression, and survival. To determine whether serum NFL at baseline in de novo PD predicts motor decline, differentially impacts specific motor features, predicts cognitive decline, and predicts loss of dopamine terminals, here we evaluated 376 de novo PD patients from the PPMI database and analyzed the effect of baseline serum NFL levels on progression over eight years of motor impairment measured with the UPDRS, cognitive function measured with the MoCA, and putamen dopamine transporter (DAT) binding ratio measured with DaTscan. In longitudinal mixed effects models that controlled for age, gender, disease duration, and levodopa equivalent drug dose, higher levels of serum NFL at baseline were associated with greater increases of UPDRS-III and total UPDRS scores, with greater worsening of postural instability and gait disorder (PIGD) scores but not tremor scores over time. In contrast, baseline serum NFL was not associated with significant progression of MoCA scores in this de novo PD cohort. Higher baseline serum NFL was associated with greater reduction of putamen DAT binding ratio over time. Together, these findings show that baseline serum NFL levels predict the rate of motor decline, the accumulation of PIGD clinical features, and the progression of dopamine transporter loss in the early stage of PD.

*Corresponding author. Department of Neurology Building 114, 16th Street, Suite 2004, Charlestown, MA, 02129-4404, USA. gomperts.stephen@mgh.harvard.edu (S.N. Gomperts). **Corresponding author. Department of Neurology, 88 Jiefang Rd, Hangzhou, Zhejiang, 310009, China. brzhang@zju.edu.cn (B. Zhang).

Author roles

RY: Project execution, statistical analysis, manuscript writing and review; JL: Statistical analysis, manuscript review; AG, MQ: Manuscript review; BZ: manuscript review; SG: Project conception, project organization, manuscript writing and review.

Appendix A. Supplementary data

Supplementary data to this article can be found online at https://doi.org/10.1016/j.parkreldis.2021.02.008.

Keywords

Neurofilament light chain; Parkinson's disease; Dopamine transporter uptake; Motor decline; PIGD; Longitudinal study

1. Introduction

Fluid analytes that reflect severity and progression of idiopathic Parkinson's disease (PD) have long been sought to guide clinical decision making and clinical trials. To this end, neurofilament light chain (NFL) has been proposed as a sensitive biomarker of neuroaxonal injury in various neurological disorders, including Alzheimer's disease, frontotemporal dementia, amyotrophic lateral sclerosis, cerebral small vessel disease and multiple sclerosis [1]. Although serum NFL levels are elevated in atypical parkinsonian disorders compared to PD [2], higher NFL concentrations in PD in blood or cerebrospinal fluid have been associated with greater disease severity, shorter survival, and higher risk of progression of motor and cognitive impairments [3,4].

Recent work examining the impact of NFL on progression of PD has found that NFL predicts progression specifically in the postural instability gait disorder (PIGD) subtype of PD [5], a clinical variant associated with poorer prognosis and cognitive impairment [6]. As patients often transition between PIGD and tremor subtypes over time [7–9], however, it remains possible that NFL has prognostic value in predicting the rate of progression of PIGD clinical features in all PD patients, regardless of their dominant clinical features.

Dopamine transporter (DAT) imaging [10] provides an antemortem measure of the integrity of nigrostriatal dopaminergic terminals that are lost in PD. Although reduced DAT uptake in the putamen correlates with the severity of motor impairment, including all cardinal motor symptoms except tremor [11], DAT uptake and motor function can dissociate, for example in the context of optimized dopamine replacement therapy, as well as due to variance in duration of disease at the group level, and in the clinical assessment of motor function. Recent studies have investigated the potential association between DAT uptake and NFL levels cross-sectionally, but the results have been inconsistent [3,12]. Despite the value of this biomarker of dopamine system integrity, the relationship between baseline NFL and longitudinal decline of DAT uptake has not yet been evaluated.

To address these knowledge gaps, here we sought to determine in patients with de novo PD followed for up to 8 years in the PPMI database whether serum NFL levels at baseline predict (1) progression of motor disability overall, (2) progression of PIGD versus tremor clinical features, (3) progression of global cognitive function, and (4) change in dopamine transporter (DAT) uptake over time.

2. Methods

2.1. Participants

The participants of this study were recruited into the Parkinson Progression Markers Initiative (PPMI) database (available at http://www.ppmi-info.org). All recruited participants

were designed to have follow-up examinations each year after their baseline visit. The PPMI study was approved by the Institutional Review Board of all participating sites; all participants provided written informed consent before inclusion.

In this study, 376 de novo PD patients with available serum NFL data at baseline and with two or more visits were included. Four percent of subjects had two timepoints of non-missing data; 3.5% had three time points; 6.4% had four time points; 11.4% had five time points; 15.2% had six time points; 33.2% had seven time points; 20.7% had eight time points; and 5.6% had nine time points.

2.2. Clinical assessments and dopamine transporter imaging

PD-related signs and symptoms were assessed with the Movement Disorder Society-sponsored revision of the Unified Parkinson's Disease Rating Scale (UPDRS) every year from enrollment up to 8 years. Motor function was measured with the UPDRS part 3 (UPDRS-III) in the off-state. Cognitive function was measured with the Montreal Cognitive Assessment (MoCA).

To exclude the possibility that certain clinical features at baseline might be associated with different durations of follow-up in the study, PD participants were classified into short and long follow-up subgroups by median split of their maximum follow-up years (median, 6 years): If the maximum follow-up time was no more than 6 years, the subject was classified into the short follow-up subgroup. Otherwise, the subject was classified into the long follow-up subgroup. Baseline age, gender, disease duration, total UPDRS and UPDRS-III scores were identical between the two subgroups ($p > 0.05$, Supplementary Table 1). Subsequent analyses were performed on the entire dataset.

PIGD scores and tremor scores were computed according to previously defined criteria [13]. Briefly, the PIGD measure includes five items, which are freezing, walking and balance in UPDRS part 2 (UPDRS-II), and gait, freezing of gait, and postural stability in UPDRS-III; the tremor measure includes 11 items, which are tremor in UPDRS-II, and postural tremor, kinetic tremor, rest tremor and rest constancy in UPDRS-III. The ratio of tremor score to PIGD score was used to define tremor-dominant (TD) patients (ratio ≥ 1.15; N = 264), indeterminate patients ($0.9 <$ ratio < 1.15, N = 43) and PIGD-dominant patients (ratio ≤ 0.90, N = 69) [13]. The percentages of patients in each motor subtype at baseline and during the follow-up period are shown in Supplementary Table 2. Akinetic-rigid scores were computed by adding eight items including rigidity, finger tapping, hand movements, pronation-supination movements of hands, toe tapping, leg agility, arising from chair, and body bradykinesia in UPDRS-III [14].

DaTscan SPECT images were acquired at enrollment and in follow-up years one, two, and four. 355 participants had at least two DaTscan SPECT images. DAT binding ratios in the putamen were calculated as the count density in the putamen divided by that of the occipital cortex, which served as reference region. All participants were free of anti-parkinsonism drugs at enrollment, and levodopa equivalent drug dose (LEDD) was calculated at each follow-up visit [15]. Disease duration was defined as the duration at enrollment since the onset of symptoms. Serum NFL levels at baseline were measured with the Simoa Human

NF-light Advantage kit by using the Single Molecule Array in a fully automated SIMOA® HD-1 analyzer (Quanterix, Lexington, MA, USA). Additional details about processing of the samples can be found in the PPMI biologic manual (http://www.ppmi-info.org).

2.3. Statistical analyses

All clinical, serum NFL, CSF NFL, and neuroimaging data included in this study were simultaneously downloaded from the PPMI database on June 30, 2020. Correlations between serum NFL levels and clinical measurements at baseline were assessed via Spearman correlation analysis. Differences of serum NFL levels by sex were compared with the Wilcoxon rank sum test. To analyze the effect of serum NFL on motor progression, longitudinal mixed effects analysis was performed for the dependent variable of motor severity, reflected by different measurements including UPDRS-III scores, total UPDRS scores, PIGD scores, tremor scores, or akinetic-rigid scores, each in a separate analysis. Model selection was based on limited backward stepwise elimination ($p > 0.05$ for removal from the model), in which we ran pretest checks on fixed covariates and higher order interactions, and in which we removed them if they showed only chance relations and therefore were not confounders. The primary fixed effect predictors were levels of serum NFL at baseline, years in the study, and their interactions. The fixed covariates included sex, age at baseline, disease duration at baseline, their interactions with years in the study, and time varying LEDD. An intercept term and linear rate of change across time per subject were the random terms for the mixed effects model. For the purpose of analyzing the effect of serum NFL on changes of DAT uptake deficits, we ran the same longitudinal mixed effects model for the dependent variable of DAT uptake. As before, only those covariates reaching statistical significance were considered as confounders and were included in the final models.

To analyze the relationship between change in DAT uptake and change in motor function across time, we performed a longitudinal mixed effects analysis for the time-varying dependent variable of motor features, reflected by different measurements including total UPDRS, UPDRS-III, PIGD, tremor, and akinetic-rigid scores, each in a separate analysis. Time-varying DAT binding ratio in putamen was included as the primary fixed effect predictor. Years in the study, sex, baseline age and disease duration, their interactions with years in the study, and time varying LEDD were included as the fixed covariates. By controlling for years in the study in the model in addition to DAT uptake, we excluded the possible emergence of a spurious relation of time-varying DAT uptake to the dependent variable that is solely the result of each of these variables independently changing across time but being otherwise statistically unrelated. The random terms for the mixed effects model included an intercept term and linear rate of change across time per subject.

To analyze the effect of serum NFL levels on cognitive function over time, we performed a longitudinal mixed effects analysis for the dependent variable of MoCA scores. Levels of serum NFL at baseline, years in the study, and their interaction were included as the primary fixed effect predictors. Age and disease duration at baseline, sex, years of education, their interactions with years in the study, and time varying treatment for cognitive dysfunction with acetylcholine esterase inhibitors were included as the fixed covariates. Once again, an

intercept term and linear rate of change across time per subject were the random terms for the mixed effects model. We also ran a statistical analysis for CSF NFL levels similar to those involving the serum NFL levels. Given the lower sample size of de novo PD subjects with CSF samples, this study focused on the relation of serum NFL levels to progression of motor features.

Residuals from model fixed effect predictions and combined fixed and random predictions were checked for conformance to normality assumptions. A value of $p < 0.05$ was considered statistically significant. Standard error is reported unless stated otherwise. Statistical analysis was performed in R software (version 3.6.3, available at http://www.r-project.org).

3. Results

3.1. Demographic and clinical features

The demographic and clinical features of all 376 de novo PD participants are shown in Table 1. The average age at baseline was 62.2 ± 9.8 years (SD), and the percentage of males was 63.8%. PD patients were newly diagnosed and drug naïve, with mean duration since symptom onset of 2.0 ± 2.0 years (SD). The average follow-up time was 5.7 ± 1.6 years (SD).

At baseline, serum NFL concentrations positively correlated with age (rho = 0.60, $p < 0.001$) but did not differ by sex ($p = 0.6$). No association was detected between serum NFL levels and disease duration (rho = 0.04, $p = 0.5$). Higher levels of serum NFL were associated with more severe parkinsonism, as measured by total UPDRS scores and UPDRS-III scores (total UPDRS: rho = 0.17, $p < 0.001$; UPDRS-III: rho = 0.16, $p = 0.001$). Higher levels of serum NFL were also associated with greater cognitive impairment, as measured by MoCA scores (rho = −0.21, $p < 0.001$). In this cohort, serum NFL levels at baseline were not significantly associated with the putamen DAT binding ratio, and only a weak negative trend was observed (rho = − 0.09, $p = 0.092$).

3.2. Predictive effects of baseline serum NFL levels on the rate of PD-related functional decline

In longitudinal analysis, elevated levels of serum NFL at baseline were associated with a significantly faster increase in UPDRS-III scores over 8 years ($p = 0.003$). Similar results were found for total UPDRS scores ($p < 0.001$). For each increase of 10 pg per milliliter (pg/ml) in serum NFL at baseline, UPDRS-III scores and total UPDRS scores climbed each year by 0.52 ± 0.17 points and 0.96 ± 0.28 points, respectively (Fig. 1A and B). Interestingly, compared to females, males had a steeper increase of UPDRS-III and total UPDRS scores over time (UPDRS-III, $p = 0.024$; total UPDRS scores: $p = 0.005$), with an approximate growth of 0.54 ± 0.24 excess points for UPDRS-III scores and 1.10 ± 0.38 excess points for total UPDRS scores per year in males compared to females.

3.3. Predictive effects of baseline serum NFL levels on accumulation of PD motor features

To determine whether baseline serum NFL might differentially predict progression of specific clinical features of this de novo PD cohort, we next evaluated the impact of baseline serum NFL levels on progression of PIGD scores, tremor scores, and akinetic-rigid scores. Interestingly, higher levels of serum NFL at baseline were associated with a faster increase of PIGD scores over 8 years ($p < 0.001$), with an elevation of 2.46 ± 0.43 points per decade in patients with a 10 pg/ml increase of serum NFL at baseline (Fig. 1C). In contrast, serum NFL levels at baseline were not associated with progression of tremor scores. Higher levels of serum NFL at baseline were associated with a faster increase of akinetic-rigid scores over time ($p = 0.006$, Supplementary Fig. 1), but this association was not significant in the initial model when controlling for all covariates.

We next set out to evaluate whether the NFL-associated accumulation of PIGD impairments was restricted to PIGD-dominant patients defined at baseline (see Methods) or was a more general finding in the de novo PD cohort. Within the PIGD-dominant subgroup but not the tremor-dominant subgroup, higher baseline NFL levels predicted faster increases of total UPDRS and UPDRS-III scores (total UPDRS: $p = 0.006$; UPDRS-III: $p = 0.006$). However, in both PIGD-dominant and tremor-dominant subgroups, higher baseline NFL levels were associated with faster worsening of PIGD scores (PIGD subgroup: $p < 0.001$; TD subgroup: $p = 0.039$). In contrast, and as expected from the analyses above, baseline NFL levels were not associated with worsening tremor scores in either subgroup. Thus, the impact of baseline NFL on PIGD impairments was not subtype specific and appeared to affect the de novo PD cohort more broadly.

3.4. Predictive effects of baseline serum NFL levels on the rate of cognitive decline

We built a mixed effects longitudinal model to evaluate whether baseline serum NFL levels could predict the progression of cognitive impairment in this cohort of de novo PD patients. We found that levels of serum NFL at baseline were not significantly associated with the rate of cognitive decline as measured by MoCA scores over time ($p = 0.15$).

3.5. Associations between baseline serum NFL level and progressive reduction of DAT uptake

To evaluate whether baseline serum NFL level predicted deterioration of striatal dopamine, we next investigated NFL's effects on longitudinally acquired putamen DAT binding ratio. Compared to the original cohort, and to those without at least two DAT scans ($N = 21$), participants who underwent at least two DAT scans ($N = 355$) had comparable age, sex, disease duration and baseline UPDRS scores ($p > 0.05$ for each contrast, Supplementary Table 3). The average follow-up time for DAT scans was 3.5 ± 1.0 years. Although there was no significant cross-sectional association detected between serum NFL levels and putamen DAT binding ratio at baseline, as noted above, higher levels of serum NFL at baseline were associated with a steeper decline of putamen DAT binding ratio over time ($p = 0.013$). In this mixed-effects model, for each 10 pg/ml increase in serum NFL at baseline, putamen DAT binding ratio decreased by 0.14 ± 0.06 units per decade (Fig. 1D).

Given the association of baseline serum NFL levels with both worsening motor function and decline in DAT binding ratio over time, we next examined the relationship between changes in DAT binding over time and changes in motor function. Greater loss of DAT binding over time was associated with greater increases of UPDRS-III and total UPDRS scores (both $p < 0.001$), and specifically with greater increase of akinetic-rigid scores ($p < 0.001$), but not with changes in PIGD ($p = 0.19$) or tremor ($p = 0.8$) scores.

Of note, all of the key results that were significant after backward elimination in this longitudinal study were significant in the initial full model unless otherwise noted. Residuals from fixed and random predicted values reasonably conformed to normality assumptions for all longitudinal models.

3.6. Exploratory findings of CSF NFL levels in de novo PD patients

Among all 376 subjects in the study, only 207 (55%) had CSF NFL levels at baseline (Supplementary Table 4). These were evaluated on an exploratory basis in the Supplement. Serum NFL and CSF NFL were strongly correlated ($N = 207$, rho = 0.63, $p < 0.001$). Results with CSF NFL levels were broadly similar to those with serum NFL (Supplementary Fig. 2).

4. Discussion

In this eight-year longitudinal study of de novo PD, baseline serum NFL levels were found to predict decline in overall motor function, worsening of PIGD clinical features but not tremor, and loss of putamen DAT over time. Consistent with previous cross-sectional studies, NFL levels were found to correlate with baseline UPDRS-III scores [3,16,17]. Thus, NFL levels appear to reflect neuronal injury in de novo PD. While some previously reported longitudinal studies of NFL have found higher levels of NFL in blood or CSF to be associated with increased risk of PD motor progression [4], others have found only a trend correlation [18]. By employing a longitudinal design with dynamic analyses of clinical features, evaluating 8 years of longitudinal data compared to up to 3 years in previous studies, and restricting analyses to de novo PD with short (average, 0.6 years) duration of disease (compared to > 1 year in previous studies), we were able to demonstrate that a 10 pg/ml increase in serum NFL level at baseline in PD is associated with an increase of UPDRS-III score of 5 points per decade.

Interestingly, the effect of baseline NFL on progression of global motor impairments indexed with the UPDRS-III was reflected in a similar effect of baseline serum NFL on progression of PIGD clinical impairments, with a trend towards progression of akinetic-rigid impairments as well, but with no effect on progression of tremor. Few studies to date have investigated the associations between NFL and PIGD features, cross-sectionally [3,12] or longitudinally [5]. In a recent longitudinal study, serum NFL at baseline was associated with faster motor decline in a subgroup of patients with the PIGD subtype but not the tremor-dominant subtype defined at baseline [5]. Consistent with evidence of motor subgroup transitions in de novo PD [8] and with longer follow-up times [7], we found that while only 18.4% of patients could be classified into the PIGD subtype at baseline, PIGD clinical features evolved in relation to baseline NFL in the entire cohort and could be detected in both the PIGD-dominant subgroup as well as the tremor-dominant subgroup.

As PIGD symptoms are linked to Hoehn and Yahr motor progression and have been closely associated with cognitive impairment in PD [7,19,20], the prognostic value of serum NFL for progression of PIGD symptoms may find utility in clinical trials targeting these patients in the early stage.

To our knowledge, this is the first observation linking NFL levels at baseline to loss of putamen DAT binding ratio over time in PD. This result suggests that neuroaxonal injury reflected in baseline NFL levels and detected at the early phase of disease is a relevant correlate of subsequent rate of dopaminergic neurodegeneration. Of note, the present results linking serum NFL to clinical course in PD are supported by cross-sectional studies where NFL levels in blood and CSF have been found to strongly correlate (r value in the current study of 0.6) [21], and where NFL levels in CSF have been observed to correlate with striatal DAT levels cross-sectionally [3]. It is intriguing that serum NFL has sensitivity for such progression. Together with the observation that changes in DAT binding over time were associated with progression of akinetic-rigid features rather than PIGD or tremor features, supported by prior cross-sectional and longitudinal results linking striatal DAT binding ratio to bradykinesia and rigidity in PD [22–24], these results suggest that loss of nigrostriatal integrity may contribute to the observed association between baseline NFL level and motor progression in PD primarily through its effects on bradykinesia and rigidity.

Limitations of this study include the lack of neuropathological diagnoses of participants with de novo PD. However, reduced striatal DAT uptake on DaTscan increases confidence of the clinical diagnosis of PD in this multi-center clinical study. Although the presence of some missing data in the dataset might have influenced the results, the mixed effects models built in our statistical analyses permitted reasonable estimates of effects in spite of some missing timepoints for some subjects, maximized use of available data, and optimized the power of the analyses [25]. In addition, we found no evidence for differential drop-out of subjects on the basis of baseline clinical features that could contribute to our observations, as baseline demographic and clinical features were comparable in the short follow-up de novo PD subgroup and the long follow-up subgroup. Another limitation is the lack of detailed cognitive testing that reduced sensitivity to detect an effect of NFL on changes in cognitive function over time, although we were able to detect a cross-sectional association between higher NFL levels with lower MOCA scores, as shown previously [4,12,26]. Strengths of this study include the long follow-up period, the relatively large sample size, and the study of a de novo PD cohort, which reduced heterogeneity in baseline disease severity and duration. In addition, multiple features of our mixed effects models touched base with prior observations, including the linear increase in UPDRS scores over time [27].

5. Conclusions

Baseline serum NFL levels in de novo PD predict decline in overall motor function, in PIGD features specifically, and in putamen DAT levels reflecting nigrostriatal dopamine neuropathology over an 8-year period. Given these findings and its ease of acquisition, serum NFL is likely to have value as a biomarker in PD clinical trials, with potential, for example, to discriminate fast from slow progressors. Further studies to understand the pathophysiological mechanisms of NFL as a predictive PD biomarker are needed.

Supplementary Material

Refer to Web version on PubMed Central for supplementary material.

Acknowledgements

The authors thank all the participants recruited in this study. Data used in the preparation of this article were obtained from the Parkinson's Progression Markers Initiative (PPMI) database (https://www.ppmi-info.org/data). For up-to-date information on the study, visit https://www.ppmi-info.org.

Funding

Department of Defense CDMRP/W81XW1810516, NINDS 1R21 NS109833, Lewy Body Dementia Association Research Centers of Excellence Program.

Declaration of competing interest

RY, JL, AG, MQ, BZ have nothing to disclose. SG serves on an Advisory Board for Acadia Pharmaceuticals. He receives funding from NIH grant R01 AG054551, P50 AG005134, R21 NS109833, DOD CDMRP/W81XW1810516, the Farmer Family Parkinson's Initiative, and the Lewy Body Dementia Association. None of the authors of this manuscript has any potential conflict of interest related to the content of this study.

References

[1]. Khalil M, Teunissen CE, Otto M, Piehl F, Sormani MP, Gattringer T, Barro C, Kappos L, Comabella M, Fazekas F, Petzold A, Blennow K, Zetterberg H, Kuhle J, Neurofilaments as biomarkers in neurological disorders, Nat. Rev. Neurol 14 (10) (2018) 577–589. [PubMed: 30171200]

[2]. Marques TM, van Rumund A, Oeckl P, Kuiperij HB, Esselink RAJ, Bloem BR, Otto M, Verbeek MM, Serum NFL discriminates Parkinson disease from atypical parkinsonisms, Neurology 92 (13) (2019) e1479–e1486. [PubMed: 30814322]

[3]. Backstrom D, Linder J, Jakobson Mo S, Riklund K, Zetterberg H, Blennow K, Forsgren L, Lenfeldt N, NfL as a biomarker for neurodegeneration and survival in Parkinson disease, Neurology 95 (7) (2020) e827–e838. [PubMed: 32680941]

[4]. Lin CH, Li CH, Yang KC, Lin FJ, Wu CC, Chieh JJ, Chiu MJ, Blood NfL: a biomarker for disease severity and progression in Parkinson disease, Neurology 93 (11) (2019) e1104–e1111. [PubMed: 31420461]

[5]. Ng ASL, Tan YJ, Yong ACW, Saffari SE, Lu Z, Ng EY, Ng SYE, Chia NSY, Choi X, Heng D, Neo S, Xu Z, Keong NCH, Tay KY, Au WL, Tan LCS, Tan EK, Utility of plasma Neurofilament light as a diagnostic and prognostic biomarker of the postural instability gait disorder motor subtype in early Parkinson's disease, Mol. Neurodegener 15 (1) (2020) 33. [PubMed: 32503574]

[6]. van der Heeden JF, Marinus J, Martinez-Martin P, Rodriguez-Blazquez C, Geraedts VJ, van Hilten JJ, Postural instability and gait are associated with severity and prognosis of Parkinson disease, Neurology 86 (24) (2016) 2243–2250. [PubMed: 27178702]

[7]. Alves G, Larsen JP, Emre M, Wentzel-Larsen T, Aarsland D, Changes in motor subtype and risk for incident dementia in Parkinson's disease, Mov. Disord 21 (8) (2006) 1123–1130. [PubMed: 16637023]

[8]. Simuni T, Caspell-Garcia C, Coffey C, Lasch S, Tanner C, Marek K, Investigators P, How stable are Parkinson's disease subtypes in de novo patients: analysis of the PPMI cohort? Park. Relat. Disord 28 (2016) 62–67.

[9]. Eisinger RS, Martinez-Ramirez D, Ramirez-Zamora A, Hess CW, Almeida L, Okun MS, Gunduz A, Parkinson's disease motor subtype changes during 20 years of follow-up, Park. Relat. Disord 76 (2020) 104–107.

[10]. Eshuis SA, Jager PL, Maguire RP, Jonkman S, Dierckx RA, Leenders KL, Direct comparison of FP-CIT SPECT and F-DOPA PET in patients with Parkinson's disease and healthy controls, Eur. J. Nucl. Med. Mol. Imag 36 (3) (2009) 454–462.

[11]. Benamer HT, Patterson J, Wyper DJ, Hadley DM, Macphee GJ, Grosset DG, Correlation of Parkinson's disease severity and duration with 123I-FP-CIT SPECT striatal uptake, Mov. Disord 15 (4) (2000) 692–698. [PubMed: 10928580]

[12]. Sampedro F, Perez-Gonzalez R, Martinez-Horta S, Marin-Lahoz J, Pagonabarraga J, Kulisevsky J, Serum neurofilament light chain levels reflect cortical neurodegeneration in de novo Parkinson's disease, Park. Relat. Disord 74 (2020) 43–49.

[13]. Stebbins GT, Goetz CG, Burn DJ, Jankovic J, Khoo TK, Tilley BC, How to identify tremor dominant and postural instability/gait difficulty groups with the movement disorder society unified Parkinson's disease rating scale: comparison with the unified Parkinson's disease rating scale, Mov. Disord 28 (5) (2013) 668–670. [PubMed: 23408503]

[14]. Kang GA, Bronstein JM, Masterman DL, Redelings M, Crum JA, Ritz B, Clinical characteristics in early Parkinson's disease in a central California population-based study, Mov. Disord 20 (9) (2005) 1133–1142. [PubMed: 15954133]

[15]. Tomlinson CL, Stowe R, Patel S, Rick C, Gray R, Clarke CE, Systematic review of levodopa dose equivalency reporting in Parkinson's disease, Mov. Disord 25 (15) (2010) 2649–2653. [PubMed: 21069833]

[16]. Hansson O, Janelidze S, Hall S, Magdalinou N, Lees AJ, Andreasson U, Norgren N, Linder J, Forsgren L, Constantinescu R, Zetterberg H, Blennow K, F. s. Swedish Bio, Blood-based NfL: a biomarker for differential diagnosis of parkinsonian disorder, Neurology 88 (10) (2017) 930–937. [PubMed: 28179466]

[17]. Lerche S, Wurster I, Roben B, Zimmermann M, Machetanz G, Wiethoff S, Dehnert M, Rietschel L, Riebenbauer B, Deuschle C, Stransky E, Lieplt-Scarfone I, Gasser T, Brockmann K, CSF NFL in a longitudinally assessed PD cohort: age effects and cognitive trajectories, Mov. Disord 35 (7) (2020) 1138–1144. [PubMed: 32445500]

[18]. Mollenhauer B, Dakna M, Kruse N, Galasko D, Foroud T, Zetterberg H, Schade S, Gera RG, Wang W, Gao F, Frasier M, Chahine LM, Coffey CS, Singleton AB, Simuni T, Weintraub D, Seibyl J, Toga AW, Tanner CM, Kieburtz K, Marek K, Siderowf A, Cedarbaum JM, Hutten SJ, Trenkwalder C, Graham D, Validation of Serum Neurofilament Light Chain as a Biomarker of Parkinson's Disease Progression, Mov Disord, 2020.

[19]. Burn DJ, Rowan EN, Allan LM, Molloy S, O'Brien JT, McKeith IG, Motor subtype and cognitive decline in Parkinson's disease, Parkinson's disease with dementia, and dementia with Lewy bodies, J. Neurol. Neurosurg. Psychiatry 77 (5) (2006) 585–589. [PubMed: 16614017]

[20]. Blaszczyk JW, Orawiec R, Duda-Klodowska D, Opala G, Assessment of postural instability in patients with Parkinson's disease, Exp. Brain Res 183 (1) (2007) 107–114. [PubMed: 17609881]

[21]. Bacioglu M, Maia LF, Preische O, Schelle J, Apel A, Kaeser SA, Schweighauser M, Eninger T, Lambert M, Pilotto A, Shimshek DR, Neumann U, Kahle PJ, Staufenbiel M, Neumann M, Maetzler W, Kuhle J, Jucker M, Neurofilament light chain in blood and CSF as marker of disease progression in mouse models and in neurodegenerative diseases, Neuron 91 (1) (2016) 56–66. [PubMed: 27292537]

[22]. Pirker W, Correlation of dopamine transporter imaging with parkinsonian motor handicap: how close is it? Mov. Disord 18 (Suppl 7) (2003) S43–S51.

[23]. Rossi C, Frosini D, Volterrani D, De Feo P, Unti E, Nicoletti V, Kiferle L, Bonuccelli U, Ceravolo R, Differences in nigro-striatal impairment in clinical variants of early Parkinson's disease: evidence from a FP-CIT SPECT study, Eur. J. Neurol 17 (4) (2010) 626–630. [PubMed: 20050904]

[24]. Li W, Lao-Kaim NP, Roussakis AA, Martin-Bastida A, Valle-Guzman N, Paul G, Loane C, Widner H, Politis M, Foltynie T, Barker RA, Piccini P, 11) C-PE2I and (18) F-Dopa PET for assessing progression rate in Parkinson's: a longitudinal study, Mov. Disord 33 (1) (2018) 117–127. [PubMed: 29082547]

[25]. Locascio JJ, Atri A, An overview of longitudinal data analysis methods for neurological research, Dement Geriatr Cogn Dis Extra 1 (1) (2011) 330–357. [PubMed: 22203825]

[26]. Lin YS, Lee WJ, Wang SJ, Fuh JL, Levels of plasma neurofilament light chain and cognitive function in patients with Alzheimer or Parkinson disease, Sci. Rep 8 (1) (2018) 17368. [PubMed: 30478269]

[27]. Holden SK, Finseth T, Sillau SH, Berman BD, Progression of MDS-UPDRS scores over five years in de novo Parkinson disease from the Parkinson's progression Markers initiative cohort, Mov Disord Clin Pract 5 (1) (2018) 47–53. [PubMed: 29662921]

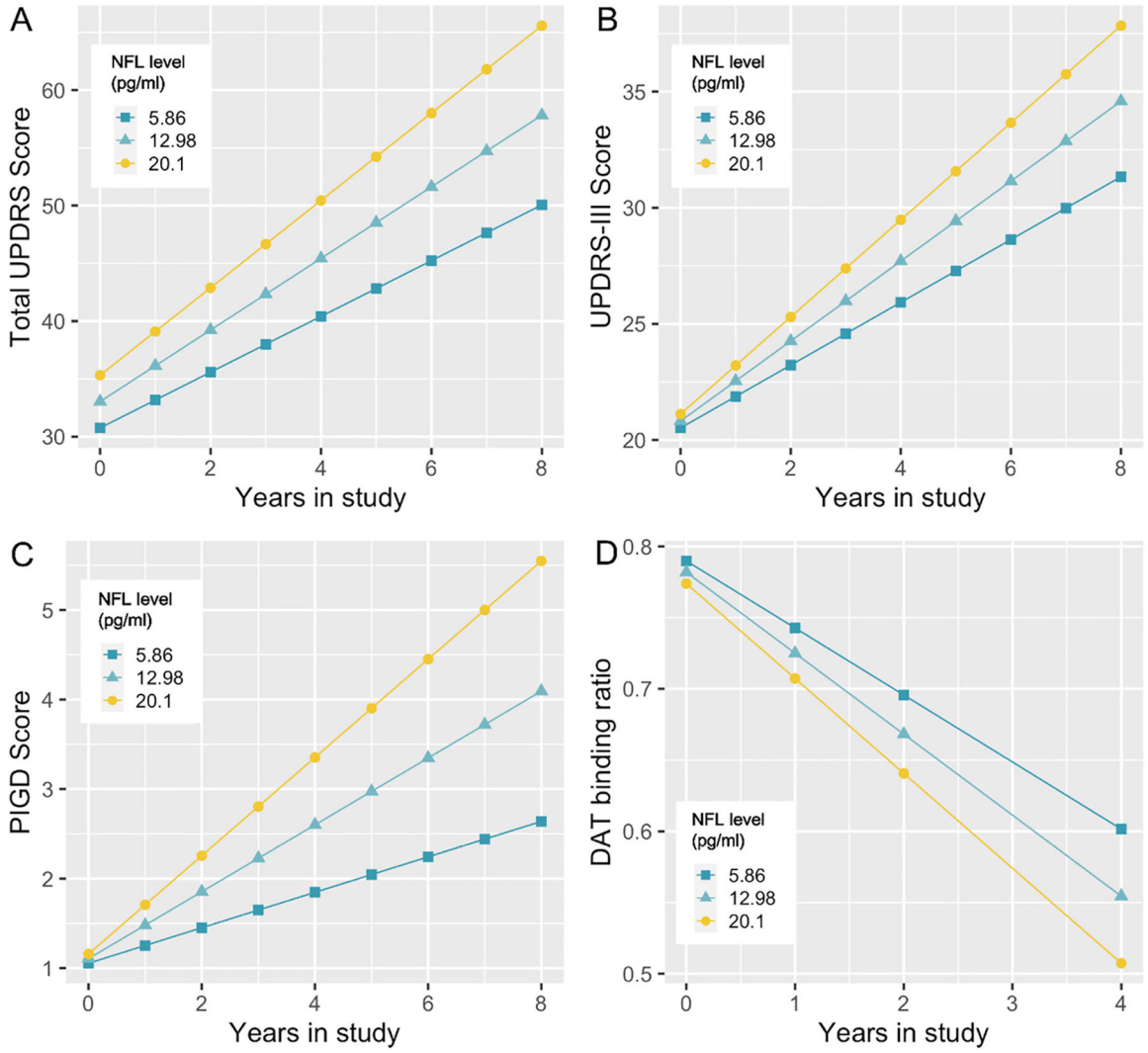

Fig. 1.

Baseline serum NFL levels in de novo PD are associated with disease progression. Predicted values from model fixed effects are shown for each of the following clinical features for three levels of baseline serum NFL (adjusted for other predictor and covariate terms): (A). Total UPDRS score; (B). UPDRS-III score; (C). PIGD score; (D). DAT binding ratio in putamen. The predictive values of NFL reflect low (1 standard deviation below mean), mean, and high (1 standard deviation above mean) levels.

Table 1

Study population demographic and clinical data at baseline.

Clinical characteristics	De novo PD
No. of individuals (N)	376
Age (mean years, SD)	62.2 (9.8)
No. of males (N, %)	240 (63.8)
Disease duration (mean years, SD)	2.0 (2.0)
Total UPDRS (mean, SD)	32.2 (13.1)
(median, range)	31 (7, 70)
UPDRS-III (mean, SD)	20.9 (8.9)””
(median, range)	20 (4, 51)
PIGD score (mean, SD)	1.1 (1.1)
(median, range)	1 (0, 6)
Tremor score (mean, SD)	5.4 (3.5)
(median, range)	5 (0, 20)
Akinetic-rigid score (mean, SD)	13.6 (7.3)
(median, range)	12 (2, 34)
MoCA (mean, SD)	27.1 (2.4)
(median, range)	27 (17, 30)
Serum NFL levels (mean pg/ml, SD)	13.0 (7.1)
(median, range)	11.5 (1.8, 76.6)
DAT binding ratio (mean, SD)	0.8 (0.3)
(median, range)[a]	0.8 (0.2, 2.2)

[a]355 participants underwent baseline DaTscan SPECT.